



Repositorio Institucional de la Universidad Autónoma de Madrid

<https://repositorio.uam.es>

Esta es la **versión de autor** del artículo publicado en:

This is an **author produced version** of a paper published in:

Chemical Communications 55.51 (2019): 7277-7299

DOI: <https://doi.org/10.1039/C9CC03166A>

Copyright: © The Royal Society of Chemistry 2019

El acceso a la versión del editor puede requerir la suscripción del recurso

Access to the published version may require subscription

Guidelines for the Assembly of Hydrogen-bonded Macrocycles

F. Aparicio,^a M. J. Mayoral,^a C. Montoro-García,^a and D. González-Rodríguez^{*a,b}

The formation of well-defined, discrete self-assembled architectures relies on the interplay between non-covalent interactions and cooperative phenomena. In particular, chelate or intramolecular cooperativity is responsible for the assembly of closed, cyclic structures in competition with open, linear oligomers, and it can be enhanced in several ways to increase the stability of a given cycle size. In this article, we review the work of several researchers in the synthesis of hydrogen-bonded macrocycles from ditopic molecules and analyze the main factors, often interrelated, that influence the equilibrium between ring and chain species. Emphasis will be set on the diverse features that can increase cyclization fidelity, including monomer geometry, template effects, conformational effects, intramolecular interactions and H-bonding pattern.

Introduction

Encoded in their structure, molecules are programmed with information to “know” what to do under a given set of conditions. Such information may come in the form of a *function* (for instance, the electronic properties of a π -conjugated semiconductor), *reactivity* toward specific compounds, *interaction* with other molecules (a substrate that is recognized by an enzyme), or *organization* (an amphiphile that self-assembles into vesicles in water). In the last two cases, where molecules communicate with other different or the same kind of molecules, the “language” through which this information is expressed is by means of **noncovalent interactions**. Non-covalent interactions are very broad in nature and binding strength.¹ They range from purely electrostatic bonds to dispersion forces, which are governed by enthalpic factors, and to hydrophobic and phase segregation effects, where the entropic contribution may become very relevant.

However, noncovalent interactions on their own cannot explain the extraordinary degree of control and selectivity found in the self-assembly of biological and synthetic systems. They are weak by themselves, but can form much more stable structures through the sum of **cooperative effects**.^{2,3} These effects arise from the interplay of two or more interactions, so that the system as a whole behaves in a different manner as it would be expected from the sum of the isolated individual interactions. Cooperative effects may be positive or negative, and can be classified in 4 main groups:⁴ 1) *Cooperative aggregation*; 2) *Allosteric cooperativity*; 3) *Chelate*

cooperativity, responsible for the *multivalency* phenomenon; and 4) *Interannular Cooperativity*.

The biological world is a shining example when it comes to the combination of noncovalent interactions and cooperative effects, which are used to define the structure of molecules, organize them, and create a wide diversity of nanosystems having particular functions.⁵ However, the complexity of natural systems hampers the assessment of specific cooperative interactions and how they are affected by molecular structure.⁴ Instead, chemists employ simpler synthetic supramolecular models to dissect and understand individual contributions to the overall free energy of the system,^{6,7} synergic effects between combined noncovalent interactions,^{8,9} the response of the system to environment changes, and possible cooperative and multivalent phenomena that may arise between the individual constituents.

One of the most commonly studied supramolecular synthetic systems comprises a molecule (**M**) that is endowed with more than one binding site and thus has the possibility to self-assemble into closed rings (cycles) or open chains (linear oligomers). This situation is often referred as *ring-chain equilibrium*, and is represented in Fig. 1.¹⁰ Under temperature, concentration or solvent conditions that enhance noncovalent binding strength (K_{inter}), self-association occurs, leading to a distribution of supramolecular oligomers of increasing size (**M_n**).^{11,12} However, depending on monomer structure and conformational flexibility, some of these oligomers may also have the possibility to form cyclic species (**cM_n**). The cyclization process can be favored over polymerization because an additional binding event (K_{intra}) takes place without increasing the molecularity of the assembly, and thus without losing translational and rotational degrees of freedom that are penalized by entropy when two species condense to form one.^{13,14} In other words, the binding event that closes the cycle is intramolecular (or “intraspecies”) and different from the rest. The cooperative effect that increases the thermodynamic stability of the ring species with respect to the linear oligomers

^a Nanostructured Molecular Systems and Materials (MSMn) group. Departamento de Química Orgánica, Facultad de Ciencias, Universidad Autónoma de Madrid, 28049 Madrid, Spain.

^b Institute for Advanced Research in Chemical Sciences (IAdChem) Universidad Autónoma de Madrid, 28049 Madrid, Spain.

See DOI: 10.1039/x0xx00000x

is defined as *chelate* or *intramolecular cooperativity*,¹⁵⁻²⁸ and it is the main factor responsible for many of the “all-or-nothing” processes found in synthetic and biological systems that produce discrete, well-defined supramolecular architectures.²⁹⁻³⁴

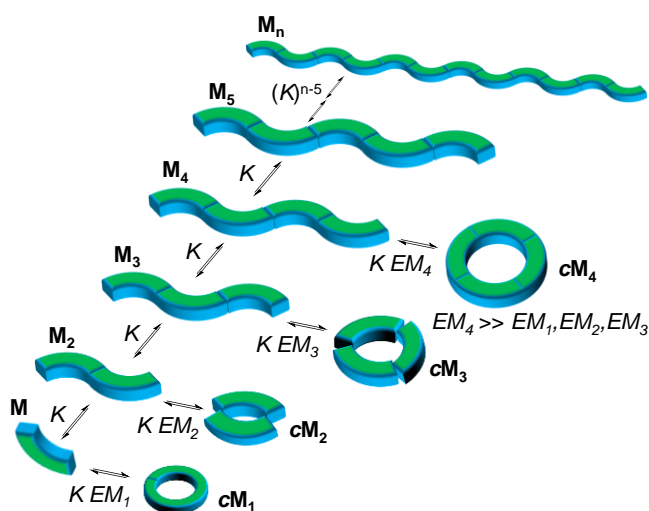


Fig. 1. Self-assembly of a molecule (**M**), having two binding sites that associates with an intermolecular equilibrium constant K , into linear (M_2 , M_3 , M_4 , M_5 ,... M_n) or cyclic (cM_1 , cM_2 , cM_3 , cM_4) structures. In this particular case, a cyclic tetramer is stabilized because the monomer and binding interaction geometric features afford a much higher EM value.

Chelate cooperativity can be quantified by the *effective molarity* (EM). For a thermodynamically controlled process, EM is defined as the ratio between the intramolecular and intermolecular equilibrium constants ($EM = K_{intra}/K_{inter}$),^{10,35-37} and can be dissected in an enthalpic and an entropic term:

$$EM = e^{-(\Delta H_{intra}^0 - \Delta H_{inter}^0)/RT} \cdot e^{(\Delta S_{intra}^0 - \Delta S_{inter}^0)/R}$$

The enthalpic component of EM may depend on electrostatic interactions or on template effects with solvent or specific guest molecules, that affect the cyclic and non-cyclic species in a different way.²⁷ Nonetheless, these effects are rare and difficult to foresee, so in most cases this component is basically related to the strain that is originated upon cyclization. It is well-recognized that monomers with a preorganized structure that afford unstrained rings are most suited to produce high EM s and thus quantitative assembly yields. In the absence of strain, the enthalpic factor becomes negligible and the EM primarily depends on entropic contributions.

The entropic component can reduce the maximum attainable EM considerably.³⁸ It depends on the symmetry and the number of components (n) of the cycle, since the reverse ring-opening reaction can take place statistically in n sites and because the EM tends to dissipate when shared among a relatively large number of molecules. Thus, the smallest non-strained macrocycles usually enjoy larger EM s than higher cyclic oligomers. The entropic contribution also depends on the degrees of freedom that are lost upon cyclization, and in particular those related to torsional and rotational motions in the cyclic *versus* linear n -mer.³⁹⁻⁴¹ It is therefore assumed that the ideal building block must be rigid and the ideal binding

interaction must be non-rotatable.^{10,37} However, if preorganization is not accurate and strain is generated because monomer and binding interaction geometries do not match for a given cycle size, flexible spacers may be preferred to produce ring structures with a small number of components (*i.e.* mostly cyclic dimers), because of the inherent entropic benefits of lower order assemblies.^{19,25}

In this Feature Article we analyze the main different aspects that affect the equilibrium between self-assembled ring and chain species,⁴² with a particular focus on the diverse factors that lead to increased cyclization fidelity. We are limiting this tutorial revision to examples found in the literature in which monocyclic species are generated from the association of two or more ditopic molecules through selective and directional hydrogen (H)-bonding interactions between donor (*D*) and acceptor (*A*) groups.⁴³⁻⁴⁵ Other excellent recent manuscripts have reviewed the self-assembly of mono- and polycyclic systems through H-bonding^{28,42,46-49} or other major supramolecular binding interactions, such as the metal-ligand coordination.^{29,32,34} We have thus collected several examples from the literature and have classified them as a function of the principal effect that influences the outcome of the cyclization process, namely: 1) monomer geometry, 2) template effects, 3) conformational effects, 4) intramolecular interactions, and 5) H-bonding pattern. It should be said that many of these factors are highly interrelated, so most of the examples presented may fall in more than one section, but we have tried to select and include in each section the most representative ones. In addition, we have tried to describe the different methods, strategies and experimental techniques that each of the many authors cited here have employed to prove the formation of cyclic assemblies, determine their dimensions and molecularity, and test their stability. We hope this work will serve as a design guide for the construction of discrete self-assembled structures, help early-stage researchers to predict, assess and characterize supramolecular cyclization processes, and contribute to a broader comprehension of chelate cooperativity.

Monomer Geometry

It is well-known that preorganization of the binding sites in a ditopic monomer toward a particular cycle shape increases cyclization yields. This is because, as explained in the introduction, chelate cooperativity is enhanced when no strain is generated (the enthalpic factor becomes negligible) and when few degrees of freedom are lost upon cyclization (the entropic contribution associated with the cyclization process is small).

Some nice examples of the impact of both effects can be found in the early work of the group of Sessler, who, as many other research groups,⁵⁰⁻⁵³ took advantage of the strong interactions between complementary natural nucleobases to direct self-association. In that context, cytosine (C) and guanine (G) derivatives have been, in general, more frequently investigated, because their H-bonding interactions are much stronger than the ones found in adenine (A) and thymidine (T) (or A-uridine (U)) pairs. For instance, in $CHCl_3$, the association constant for G:C pairs (with a triple *DDA-ADD* H-bonding

pattern) has been calculated between $K_a = 10^4$ – 10^5 M⁻¹, whereas that of A:U pairs (with a double *DA-AD* H-bonding pattern) is between $K_a = 10^2$ – 10^3 M⁻¹, that is, two orders of magnitude lower.^{54–59} In particular, Sessler *et al.* designed a series of ditopic species based on these complementary nucleobases with the aim to promote spontaneous self-assembly processes with sequence specificity (Fig. 2).^{60–63}

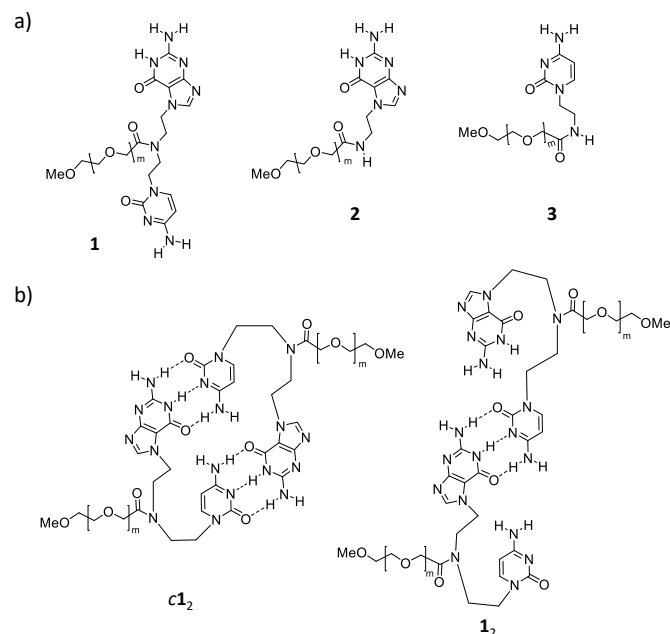


Fig. 2. (a) Chemical structure of compounds **1**, **2** and **3**. (b) Self-associated cyclic and non-cyclic structures of **1**.

Preorganization. The comparison of the association constants in DMSO-*d*₆ of the assemblies formed by the ditopic G-C molecule **1** ($K_b(\mathbf{1-1}) = 4.5$ – 6.8 M⁻¹) with the ones obtained from the association between monotopic G and C derivatives **2** and **3** ($K_b(\mathbf{2-3}) = 3.9$ – 4.7 M⁻¹), reveals a small additional binding affinity, which was ascribed to the participation of cyclic species such as **c1₂**, in addition to open H-bonded oligomers like **1₂** (Fig. 2b).⁶⁰ However, the increase in association strength is not very high, which indicates that the cyclic form is not being significantly populated. This result can be explained by the poor structural preorganization of the nucleobases in **1**, which may

generate strained macrocycles, and also by the high conformational flexibility of the spacer connecting G and C heterocycles, which brings large entropic changes to form the cyclic complexes that, consequently, would lead to low *EMs*. The authors also highlighted the poor solubility of the molecules, which is indicative of the formation of higher-order linear oligomers.⁶⁰

According to these results, the research group considered instead the use of 1,8-diethynylantracene as the spacer between complementary bases (in this case, A and U: compound **4** in Fig. 3a) to produce more rigid supramolecular structures.⁶¹ This rigid spacer orients both nucleobases to the same side of the molecule and allows for very few conformational possibilities. Upon increasing the volume fraction of DMSO-*d*₆ in CDCl₃, monomer and dimer signals were detected in slow exchange in the NMR scale (Fig. 3b). This is usually a strong indication of the formation of cyclic species that are not only thermodynamically stabilized, but also kinetically. A dimerization constant of 35 ± 5 M⁻¹ was obtained by integration of the corresponding ¹H NMR signals in 45% (v/v) DMSO-*d*₆/CDCl₃. This strong increase in the binding strength with respect to reference A and U nucleobases shows that the rigidity and preorganization of the monomer structure favours the interaction between complementary units, thus leading to rather stable cyclic systems, even when relatively weak H-bonded A:U pairs are utilized.^{60–63}

Strain. Once the influence of the rigidity of the structure in the self-dimerization process was evaluated, the same group proceeded with a comparative study of the effect of some other subtle changes in the monomer structure. For that purpose, compound **5**, with similar A-U H-bonding motifs but presenting a dibenzofuran spacer, was synthesized (Fig. 3c).⁶³ When comparing the self-assembly of **5** and **4**, some similarities and some differences should be noted. In both cases, the downfield shifts of the imide N-H protons of the U moieties observed in 100% CDCl₃ are indicative of the presence of H-bonding interactions. In contrast, such downfield shifts were not seen in DMSO-*d*₆, a strongly polar solvent that competes for H-bonding, where the monomeric species predominate for both molecules. The relative stability of the cyclic dimeric species of **4** and **5** could be compared by measuring their resistance to this polar

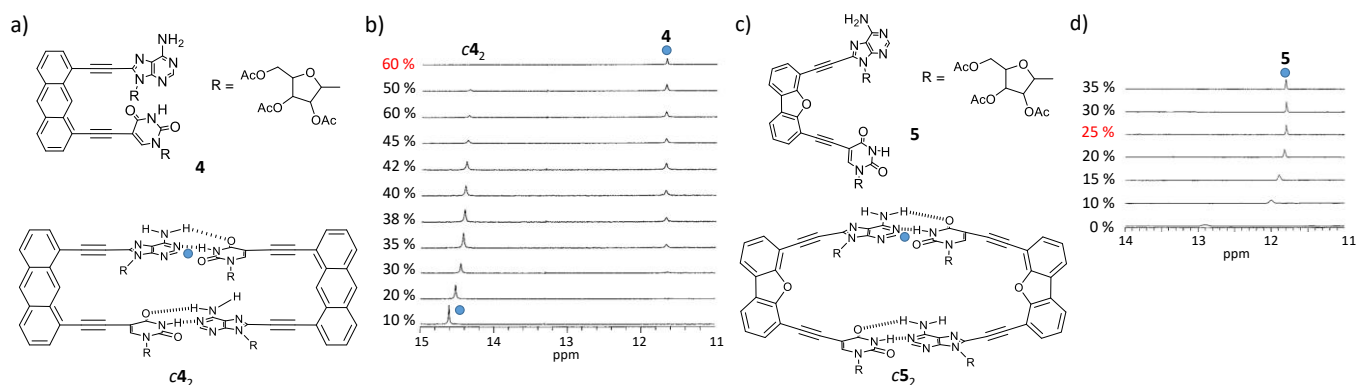


Fig. 3. A-U dinucleoside dimers **c4₂** (a) and **c5₂** (c). Changes in the ¹H NMR signals of the imide N-H proton (blue circle) of (b) **4** and (d) **5** upon increasing the volume fraction of DMSO-*d*₆ in CDCl₃. Adapted with permission from ref. 63. Copyright 1998 American Chemical Society.

cosolvent in CDCl_3 -DMSO- d_6 mixtures. Dimer $c4_2$ showed remarkable resistance and became fully dissociated when the relative DMSO- d_6 volume fraction reached 60% or higher.⁶¹ A similar experiment determined that $c5_2$ is less stable, and it could only survive 25% DMSO- d_6 . Moreover, the kinetic behaviour was also strongly affected. While the more stable dimer $c4_2$ exhibited a slow equilibrium with the monomer in the NMR timescale, as explained above, the assemblies formed by **5** were in the fast exchange regime at room temperature. The authors attributed this considerable decrease in thermodynamic and kinetic stability to the different geometric features of the aromatic spacer. Whereas the anthracene linker orients the base pairs in parallel planes and therefore presents a better predisposition to form unstrained cyclic dimers upon Watson-Crick pairing, the wider angle found in the rigid dibenzofuran spacer introduces strain in the cyclic species, which leads to a significant reduction in dimer stability.

Monomer Topology. The groups of Lehn⁶⁴ and Mascal,⁶⁵⁻⁶⁷ together with Fenniri,^{68,49} pioneered the synthesis of Janus-type molecules containing fused heterocycles with a H-bonding pattern analogous to that of G (DDA) and C (AAD) nucleobases. The rigidity of this kind of structures and the 120° angle formed between the complementary H-bonding moieties present in compounds **6a**, **6b** and **7**, allowed their self-organization into hexameric macrocyclic rosette-like species (Fig. 4).^{64,65} Such perfectly defined topology, which preorganizes the complementary H-bonding interfaces, and the absence of conformational possibilities, enhances chelate cooperativity and inhibits efficiently the formation of linear oligomers and other H-bonded species. The formation of these hexameric structures was confirmed by ^1H NMR spectroscopy and VPO (Vapour Pressure Osmometry) measurements in chloroform. Moreover, X-ray crystallographic studies indicated the presence of cyclic hexamer $c7_6$ in the solid state.⁶⁶ In the crystal structure, the $c7_6$ macrocycles overlap each other leading to a highly porous structure with an interwoven network of channels. This example is one of the few ones where X-ray single crystal analysis provide information that is consistent with the results found in solution measurements.

The supramolecular studies of this type of Janus-type motifs containing fused G^AC-like heterocycles has been more recently developed and extended by the group of Fenniri,⁶⁸ with a focus on their hierarchical organization into supramolecular rosette nanotubes (RNTs) through π - π stacking interactions between six-membered rings. Some of the latest works on this topic are focused on the design of RNTs with chiroptical^{69,70} and electron-donor behaviour.⁷¹ These authors could also enlarge the inner pore of the RNTs by introducing a 6-membered

aromatic ring between the two fused G- and C-like heterocycles.⁷² Such heterotricyclic self-complementary molecule maintained the same topology as the smaller analogue, so the fidelity of the self-assembly process into hexameric rings was not altered by this chemical modification.

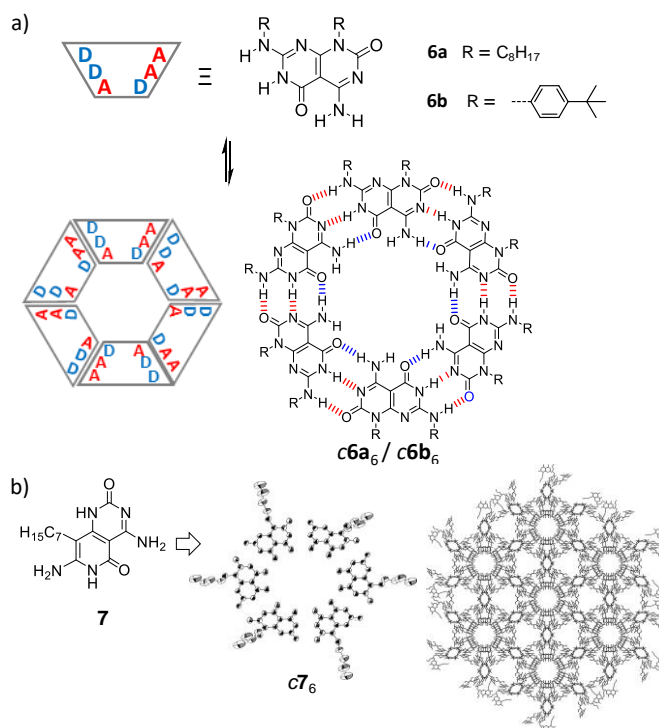


Fig. 4. (a) Proposed self-assembly of the self-complementary heterocycles **6a** and **6b** into a supramolecular macrocycle; schematic and structural representation (A/D: hydrogen acceptor/donor site). Adapted with permission from ref. 64. Copyright, 1996, Royal Society of Chemistry. (b) Oblique and cell view of the hexagonal packing of **7** in the crystal. Adapted with permission from ref. 66. Copyright, 1999, American Chemical Society.

Perrin *et al.* reported the supramolecular study of a closely related Janus-type molecule in which a central pyrrole unit was now introduced between the G^AC motif (compound **8**, Fig. 5).⁷³ The comparison of the self-assembly of compounds **6/7** and **8**, having, respectively, 6- and 4-membered rings fusing G- and C-type heterocycles with complementary H-bonding patterns, represents a beautiful example on how to rationally control cyclic assembly size from a rigid molecular topology. The self-complementary G^AC heterocycle **8** orients now the H-bonding faces of both G (ADD) and C (DAA) at a 90° angle, dictated by the geometry of the central pyrrole ring (Fig. 5a). As a consequence of this novel topology, tetrameric macrocycles containing 12 H-bonds are instead obtained from the self-association of **8**.

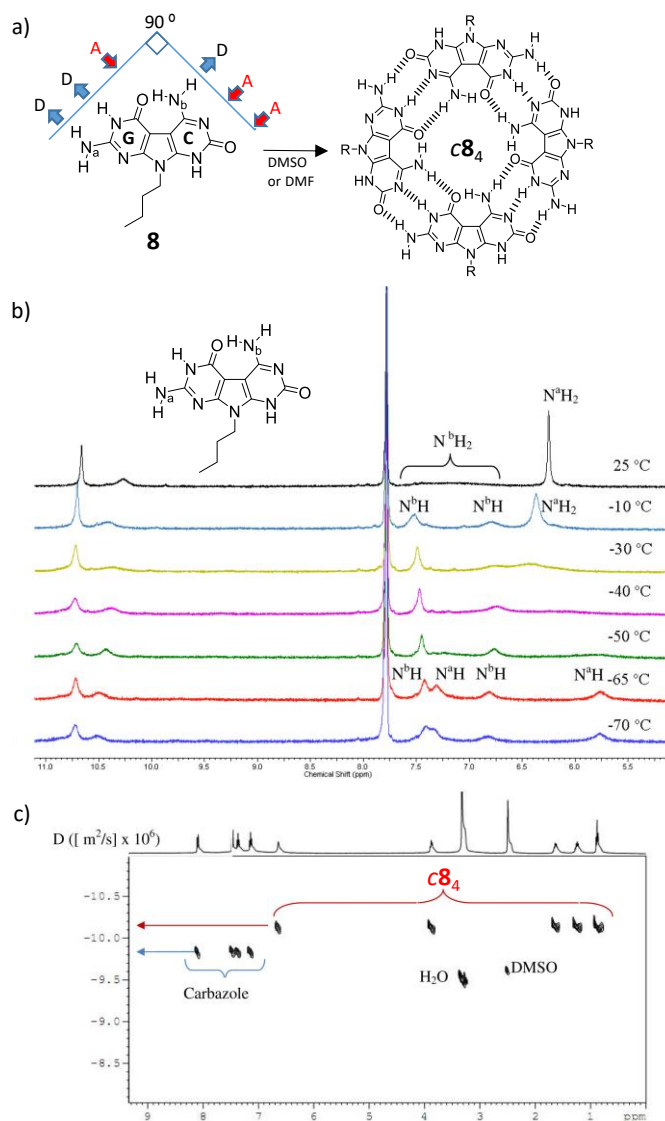


Fig. 5. (a) Monomer **G^AC 8** and the corresponding tetrameric rosette structure **c8₄**. (b) Temperature-dependent ¹H NMR experiments of **8** in DMSO-*d*₆/CDCl₃ (60/40%). (c) DOSY 2D representation of the equimolar mixture of **8** and carbazole in DMSO-*d*₆. Adapted with permission from ref. 73. Copyright, 2008, American Chemical Society.

Variable-temperature ¹H NMR experiments from 25 to 70 °C of a solution of **8** in CDCl₃-DMSO-*d*₆ mixtures (Fig. 5b) indicated the presence of H-bonds between the two complementary units. At room temperature, the NH₂ group of the G-face rotates rapidly and appears as a single peak at 6.3 ppm. In contrast, at -65 °C, rotation around the C-N bond becomes slower in the NMR timescale and the two NH₂ protons resolve as two distinct peaks at 5.75 and 7.3 ppm. On the other hand, the NH₂ protons of the C-face appear as a very broad, almost undetectable resonance at room temperature (6.75–7.65 ppm), which splits below -10 °C into two well-resolved peaks at approximately 6.8 and 7.5 ppm. These observations are consistent with a G:C pairing scheme and demonstrate the formation of the **c8₄** macrocycle. Moreover, DOSY (*Diffusion Ordered Spectroscopy*) experiments, in which the diffusion of **8** and carbazole was compared (Fig. 5c), and ESI-MS (*ElectroSpray Ionization Mass*

Spectrometry) analysis further corroborated the formation of the **c8₄** tetramer and the absence of trimeric or any other higher-order species.

Another interesting example of the regulation of cyclic aggregate structure as a function of the rigid angle between the complementary self-assembling units in the monomer was reported by de Mendoza et al.⁷⁴ In this case, the authors employed the strong DDAA–AADD quadruple H-bonding motif in the 2-ureido-4[1H]-pyrimidinone (UPy) dimers, which was initially described by Sijbesma, Meijer and co-workers,^{75,76} and nowadays used by many authors as a strategy to control self-assembly from discrete cyclic systems to supramolecular polymers in solution.^{77–80} The slight variation in the angle between the two UPy moieties in monomers **9** (109°) and **10** (120°) was controlled by the introduction of an adamantyl or a *m*-phenylene spacer, respectively (Fig. 6a). Such angle determines the preorganization of the molecules to give rise preferentially to pentameric or hexameric cycles, respectively, through the formation of 20 or 24 H-bonds between UPy units (Fig. 6b).

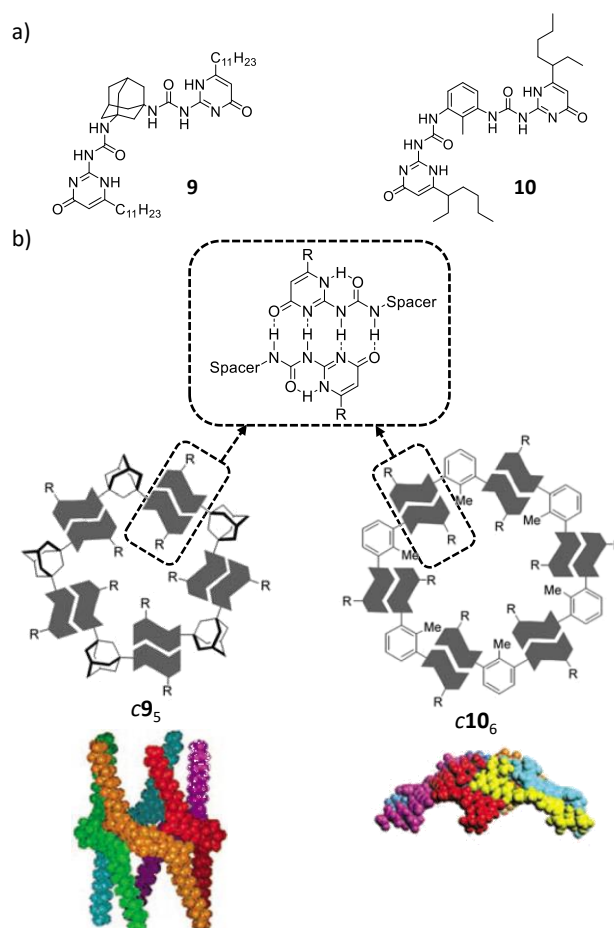


Fig. 6. (a) Structures of 1,3-adamantane and 2-methyl-1,3-phenylene bis-ureidopyrimidinones **9** and **10**. (b) Schematic and front view representations of energy-minimized of the corresponding pentameric and hexameric cyclic assemblies. Adapted with permission from ref. 74. Copyright 2005 Wiley-VCH Verlag GmbH & Co. KGaA.

ESI-MS studies indicated the presence of a high-intensity signal for the hexamer species of **10**, but signals for pentamers, tetramers, and so on, were also present in the spectrum. On the contrary, for **9**, no peaks with higher m/z than the monomer were observed. VPO and GPC (Gel Permeation Chromatography) studies seemed to confirm the formation of the expected cyclic ensembles: $c10_6$ hexamers and $c9_5$ pentamers. Additional DOSY experiments of solutions of **9** and **10** in $CDCl_3$ at different concentrations, revealed useful information about the size of the aggregates. For compound **10**, two regimes were observed: one at high concentrations in which the $c10_6$ hexamers would form high-molecular-weight structures, and other at low concentrations where the relative diffusion coefficient was smaller than the diffusion coefficient of $c9_5$. Therefore, the assemblies formed from monomer **10** must have a higher molecular weight than those formed by **9**, which is again in agreement with the hexameric and pentameric structures suggested (Fig. 6b). The higher stability of $c10_6$, relative to $c9_5$, may be ascribed to its, presumably, more flattened structure, which also allows hierarchical aggregation into higher-order-molecular-weight oligomers, as revealed by VPO and 1H NMR diffusion measurements.

Isomeric Spacers. A simple way to control ring-chain equilibria as well as the size of the cyclic assembly is to compare between rigid isomeric structures that only differ in the relative orientation of the binding motifs in a well-defined geometry.

para- and meta-phenylene isomers. Hamilton *et al.* used isomeric phenylene spacers as a reliable way to vary the angle between the interacting components in the monomer.⁸¹ As Fig. 7 shows, *meta*- and *para*-disubstituted isomers **11a** and **11b** can self-assemble into cyclic aggregates with different sizes by H-bonding interactions between carboxylate and urea moieties. Molecular modelling indicated that **11a**, disposing these moieties in a 120° angle, can form both cyclic hexamer and cyclic pentamers from the planar and nonplanar arrangements of the H-bonding groups, respectively. However, in the case of **11b**, which orient these groups in a 60° angle, cyclic trimers appear geometrically favoured with no apparent distortion of the bidentate H-bonds. The solution aggregation behaviour was studied by concentration-dependent 1H NMR experiments in $CDCl_3$, $DMSO-d_6$ - $CDCl_3$ mixtures (1:10 and 1:5) and $DMSO-d_6$. The corresponding dilution curves were analysed by a modified Saunderson and Hyne model,⁸² using different aggregation numbers. Dilution data for **11a** fitted best to the monomer-pentamer model, while a monomer-trimer model could be fitted for **11b**. In addition, these analyses indicated that the pentameric cyclic assembly of **11a** is more stable than the trimeric associate of **11b**, which was explained by the stronger Coulombic repulsion between carboxylate groups in the smaller cycle.

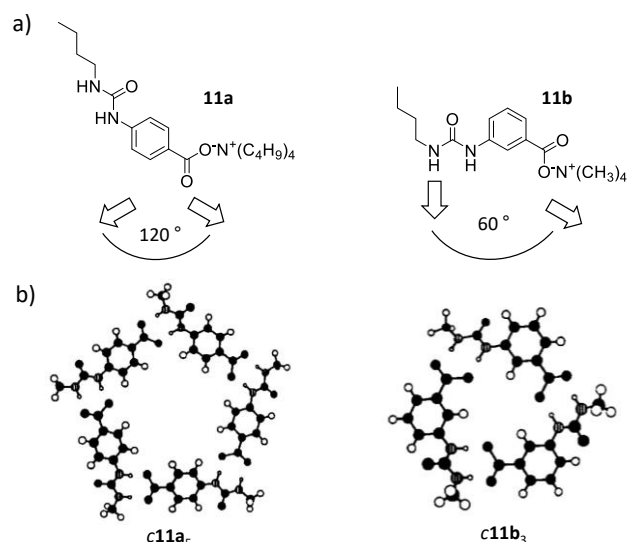


Fig. 7. (a) Structure of monomers **11a** and **11b** and (b) their corresponding pentameric and trimeric cyclic assemblies. Adapted with permission from ref. 81. Copyright 1998 Royal Society of Chemistry.

cis- and trans- Isomers. An interesting strategy for the control of the self-association process between linear and cyclic species is the use of external stimuli. Sleiman *et al.* described an example of photochemical control over the supramolecular interaction of a monomer equipped with photoresponsive units. Compounds **12a** and **12b** are two geometric isomers presenting photoswitchable azobenzene units that can generate a *trans*-*cis* photoisomerization process (Fig. 8).⁸³ In the *trans*-isomer **12a**, the formation of linear aggregates by double H-bonding association of the carboxylic acid groups is expected, due to their linear alignment in this configuration. In contrast, in the *cis*-isomer **12b** the carboxylic groups are expected to be oriented in a perpendicular fashion, allowing them to form cyclic tetramer $c12b_4$ structures (Fig. 8a).

Theoretical calculations by semiempirical PM3, DFT (Density Functional Theory; B3LYP/6-31G*), as well as ab initio (HF/6-31G*) molecular orbital calculations, corroborated the propensity of the *trans*-compound to form linear aggregates and of the *cis*-compound to assemble in cyclotetramers (Fig. 8b). Kinetic studies performed on the *cis*→*trans* thermal conversion, taking into account UV/Vis and 1H NMR data, showed a higher activation enthalpy value in $CHCl_3$ ($\Delta H^\ddagger = 97.4 \pm 4.2$ kJ mol⁻¹) than in DMSO ($\Delta H^\ddagger = 84.9 \pm 4.5$ kJ mol⁻¹), and a less negative activation entropy in $CHCl_3$ ($\Delta S^\ddagger = -15.9 \pm 13.7$ J mol⁻¹ K⁻¹) than in DMSO ($\Delta S^\ddagger = -72.8 \pm 8.0$ J mol⁻¹ K⁻¹). This data is consistent with an additional contribution to the activation energy of the *cis*→*trans* isomerization, which must be coming from the dissociation of the H-bonded closed structure, and seems to confirm the presence of discrete tetramers in $CHCl_3$ of increased stability than linear H-bound oligomers. A second level of organization is observed by TEM (Transmission Electron Microscopy) and DLS (Dynamic Light Scattering) measurements. Large sheet-like aggregates were observed for **12a** (Fig. 8c, left), in agreement with an ordered arrangement in stacked linear tapes. In contrast, the **12b** isomer formed large bundles (Fig. 8c,

right), suggesting further organization of **c12b₄** through π - π stacking and/or alky-alkyl interactions.

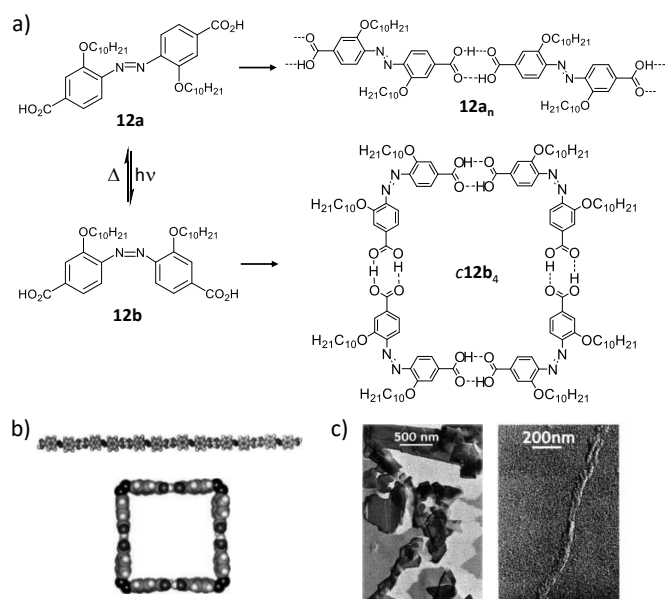


Fig. 8. (a) H-bond self-assembly of *trans*-**12a** and *cis*-**12b** azodibenzoic acid. (b) PM3-optimized geometry of a linear hexameric tape formed from **12a**, and a square formed from **12b**, respectively. (c) TEM images of **12a** (left) and **12b** (right). Adapted with permission from ref. 83. Copyright 2003 Wiley-VCH Verlag GmbH&Co. KGaA.

Template Effects

Some cycles that are formed in competition with other cycles or linear oligomers may present a central cavity that is suited, in terms of size and/or arrangement of functional groups, to accommodate other chemical species. Such guest recognition and encapsulation leads to an extra stabilization of the corresponding cyclic species *via* a template effect.

G-quartets. The G-quartet motif constitutes one of the most outstanding examples of the construction of discrete assemblies by a template effect.⁸⁴⁻⁸⁷ These species are tetrameric macrocycles that are assembled by double H-bonding (*DD-AA*) association of G derivatives through the Watson-Crick (*DD*) and Hoogsteen (*AA*) edges. This cyclic structure is usually in equilibrium with linear assemblies (G-ribbons). However, in the presence of certain cations, typically Na⁺ or K⁺ salts, the cyclic species can be additionally stabilized by cation complexation, since the quartets present four carbonyl groups pointing towards their inner cavity (Fig. 9). These quartets further tend to form stacked structures in which the complexed cation is sandwiched between two quartet layers and coordinated to 8 carbonyl groups. Such higher-order multicyclic stacked architectures are called G-quadruplexes,⁸⁴⁻⁸⁷ and are formed by a hierarchical self-assembly process, driven by a combination of π - π stacking, solvophobic and cation-dipole interactions.⁸⁸⁻⁹¹

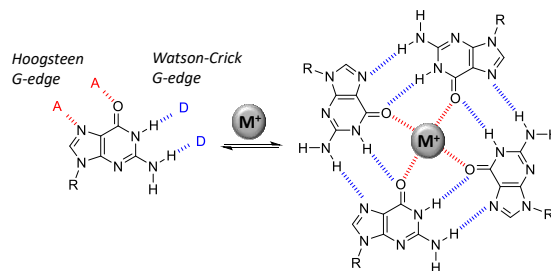


Fig. 9. Self-assembly of guanine derivatives into G-quartets templated by alkaline salts.

Nonetheless, despite the strong preference for sandwiched complexes, the stabilization and characterization of cation-free or Na⁺-bound isolated G-quartets has been achieved in a few cases in the crystal^{92,93} or gas phases,⁹⁴ or using covalent⁹⁵⁻⁹⁹ and noncovalent¹⁰⁰ templates. A simpler way to isolate G-quartet structures is to induce strong interactions between this planar macrocycle and specific substrates. This approach provides an extra stabilization of the cyclic species due to the presence of molecule-substrate interactions and the fact that the molecules are concentrated on a surface. Upon physisorption, several degrees of translational, rotational, and vibrational freedom are lost, and as a result, molecules that display very weak and ill-defined binding in solution can form well-ordered assemblies when confined in two dimensions.²⁸ In this way, several research groups have studied the formation of H-bonded supramolecular G-quartet networks onto solid surfaces and visualized them by STM (*Scanning Tunnelling Microscopy*) at the solid/liquid interface.¹⁰¹⁻¹⁰⁴

iG-quintets and quartets. Isoguanine (iG) is a non-natural nucleobase in which the exocyclic amino and carbonyl groups exchange their positions with respect to G. The comparison between the self-assembled cyclic structures of isomers G and iG represents an additional interesting example in which a slight variation in the information programmed into the monomer structure can modify the assembly process. As we commented above, G derivatives self-assemble in cyclic tetramers because the donor and acceptor interfaces are in a 90° angle to each other. However, in iG, the self-complementary *DD-AA* faces are different, and form a slightly wider angle, very close to a perfect regular pentagon, thus allowing the formation of H-bonded pentameric structures (Fig. 10a).^{105,106}

Computational calculations established, as a general rule, that the formation of iG-tetrad ion complexes is generally favoured for smaller ions, such as Li⁺, whereas larger metal ions, like K⁺ or Cs⁺, stabilize the iG-quintet structure (Fig. 10b).¹⁰⁷ However, in the absence of metal ions, the comparison of the relative stability of the quintet with that of the tetrad indicates preferential formation of the smaller iG-quartets, which should be also entropically favoured.¹⁰⁸ As a matter of fact, the formation of iG-quartets has also been described in the literature. In 1995, the group of Prof. Davis published an iG derivative that uses complementary H-bonds to self-assemble into a *C₄*-symmetric tetramer displaying extraordinary

structural stability and selective cation binding affinity.¹⁰⁹ Two years later, Seela and co-workers observed a similar behaviour in oligonucleotides containing consecutive 7-deazaisoguanine residues.¹¹⁰

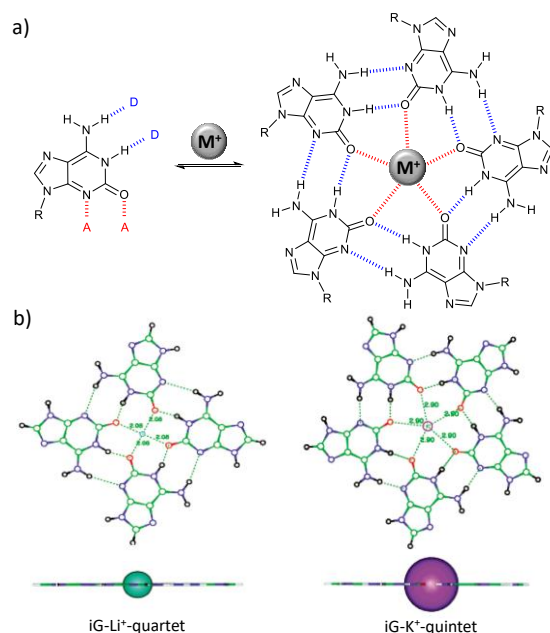


Fig. 10. (a) Isoguanine structure and assembly into iG-quintet templated by alkaline salts. (b) Calculated Structure of cyclic iG tetrad and pentad complexes with alkaline ions of different size. Adapted with permission from ref. 107. Copyright 2003 American Chemical Society.

Belt-like Assemblies. If complementary H-bonding modules that associate in a planar arrangement are fused to a curved non-planar motif, cyclic assemblies resembling to belts or capsules, rather than to planar macrocycles, can be obtained. Orentas, Butkus, Wärnmark and colleagues made use of isocytosine and UPy derivatives, that provide directional and reversible H-bonds, in combination with curved bicyclo[3.3.1]nonane central blocks, to create chiral cavities with tuneable stability, size and function.¹¹¹⁻¹¹⁵ For instance, bis-UPy molecule **13**¹¹² allowed the formation of a cyclic tetramer by quadruple H-bonding interactions between monomers (Fig. 11a). However, small variations in the 90° H-bonding angle may shift the equilibrium to the formation of larger macrocycles, like pentamers or hexamers. Solvent-controlled self-assembly was firstly checked by changing the polarity of the solvent media. Thus, ¹H NMR, DOSY NMR and GPC experiments carried out in chloroform showed the presence of cyclic tetramers exclusively, which is confirmed by MD (*Molecular Dynamics*) simulations. In contrast, in non-polar solvents like benzene or toluene, the coexistence of **c13₄** tetramers and **c13₅** pentamers was observed (Fig. 11b). These results suggest the stabilization of the tetramer cavity by the inclusion of CDCl₃ molecules, in a solvent-controlled size-selection process, while the stronger H-bonds in less polar solvents can tolerate larger distortions of the H-bonding angle, leading to larger macrocycles.

The central cavity was also used by the authors to accommodate fullerene C₆₀ as a guest. The addition of C₆₀ to a solution of compound **13** in toluene, where tetramers and pentamers are present, led to the exclusive formation of the inclusion complex C₆₀@**c13₄** (Fig 11b), monitored by the emergence of a new set of resonances in the ¹H NMR spectrum. The 1:1 binding stoichiometry between **c13₄** and C₆₀ was corroborated by the molar ratio method in titrations monitored by ¹H NMR. Moreover, the selectivity of **c13₄** toward C₆₀ and C₇₀ was studied in the same solvent by adding a 1:1 mixture of both fullerenes. ¹H NMR measurements indicated a 1:2 C₆₀:C₇₀ selectivity. The higher stability of C₇₀@**c13₄** can be explained by the larger π-surface of C₇₀, that is able to interact more strongly with the isocytosine units in compound **13** (Fig. 11b). More recently, the authors published the study of related systems that can further aggregate into tubular supramolecular polymers by establishing orthogonal H-bonding interactions,^{114,116} and in which the addition of C₇₀ guests may induce such polymerization transition.¹¹⁴

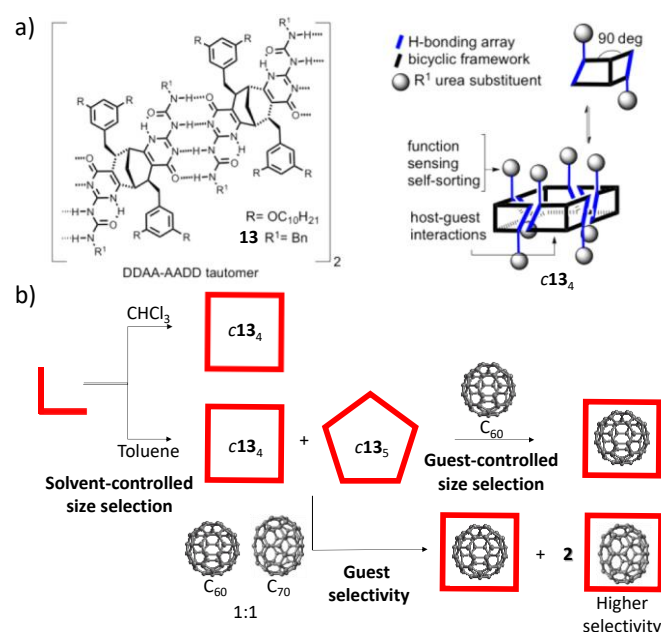


Fig. 11. (a) Chemical structure of **13** and quadruply H-bonded belt-shaped systems with an internal cavity. (b) Solvent- and guest-controlled size-selection process between **c13₄** and **c13₅**. Adapted with permission from ref. 112. Copyright 2013 American Chemical Society.

A recent study by Chamorro *et al.* also disclosed evidence for synergic relationships between H-bonded macrocycles and carbon nanomaterials, in this case (6,5)SWCNTs (Single-Walled Carbon Nanotubes).¹¹⁷ On one hand, the H-bonded rings are able to associate intimately with the SWCNTs by embracing the tube sidewalls, as confirmed by spectroscopy, microscopy and theoretical calculations, which efficiently contributes to CNT debundling and dispersion. On the other hand, SWCNTs are suitable guests for the ring cavity, and additional noncovalent interactions are established that enhance macrocycle stability. The inhibition of these reversible interactions, by adding a competing solvent for hydrogen-bonding (DMF), enabled

recovery of the CNT nanomaterial with no trace of the dispersing agent in a simple way.

Conformational Effects

Flexibility. When the linker connecting two binding sites in a ditopic monomer is rather flexible, and therefore not properly preorganized, cyclization entails a considerable entropic cost, mostly associated with the loss of rotational degrees of freedom, and thus *EM* values are frequently small. In these conditions, ring-chain equilibrium processes are particularly sensitive to the concentration. Below a critical polymerization concentration (CPC), which is related to the chelate cooperativity of the system, ring assemblies are the most abundant species. Above the CPC, polymerization starts to dominate, and the system evolves to a distribution of supramolecular polymers with an average degree of polymerization that depends on both the association constant between binding sites and the overall concentration.

For instance, bis-UPy derivatives **14a-f**,⁷⁹ containing different methyl-substituted alkyl linkers between two H-bonding UPy moieties (Fig. 12a), are not highly predisposed conformationally toward cyclization, but still preserve enough flexibility for the formation of cyclic dimers through UPy:UPy interactions at relatively low concentrations. Their corresponding critical concentration (CC), defined as the concentration where the amount of all cyclic species (dimers and others) reaches a maximum, and their cyclic dimer concentration (EDC), defined as the maximum concentration of monomer in cyclic dimers divided by 2 (the number of monomers in a cyclic dimer), allows comparing the tendency of each monomer to form cycles (Fig. 12b). These concentration values were determined by integration of the corresponding proton signals in diluted CDCl₃ solutions, where cyclic dimers are distinguishable from other assemblies.

The results shown in Fig. 12c indicate on one hand that the substitution pattern of the alkyl linkers with methyl groups determines the tendency toward cyclization of the bis-UPy derivatives. Methyl-substituted monomers **14b**, **14c**, and **14d** display an increase in EDC and CC with respect to the unsubstituted analogue **14a**, which supports the hypothesis that methyl substituents promote conformations that favour cyclodimerization. In particular, for compound **14b**, only one set of signals was observed for the UPy protons over the entire concentration range (5–300 mM), which was assigned to a cyclic

dimer, taking into account its relatively high diffusion coefficient. When **14b** and **14c** are compared, the reversal of just one stereocenter in the linker moiety leads to a dramatic increase (*i.e.* almost 10 times) in CC and EDC, an experimental result that can only be explained with a detailed analysis of the orientation of the UPy groups in the different tautomeric forms. In addition, for \pm **14b**, a pronounced selectivity between homochiral and heterochiral cyclic species was observed.⁷⁹

On the other hand, the variation of the linker length in **14d-f** led to an odd-even effect in the preference for cyclization. High EDCs were observed for monomers **14d** and **14f**, with spacers comprising 5 and 7 carbon atoms, while the EDC for **14e**, having a spacer with 6 carbon atoms, is much lower. Besides, the difference observed in EDCs of monomers **14d** and **14f** coincides with a strong change in the tautomeric form of the UPy moiety; while monomer **14d** primarily forms asymmetric cyclic dimers containing both 4[1H]-pyrimidinone and pyrimidin-4-ol tautomers, **14f** assembles in cyclic dimers almost exclusively as the 4[1H]-pyrimidinone tautomer. Overall, despite the flexibility of these molecules, the conformational preferences adopted by some of the monomers and the binding strength provided by the combined 8 H-bonds in the UPy:UPy association, results in a high preference for cyclic vs linear aggregation.

Conformational possibilities. As the linker connecting two binding sites becomes less flexible, the conformational possibilities are reduced and, if properly preorganized, *EM* (and CPC) values may increase for one or several cyclic species. Still, such semi-flexible linker may be able to adopt a few different conformations that can favour the formation of diverse cycles.

De Mendoza and co-workers designed monomers in which two UPy moieties were attached through methylene bridges to a 3,6-carbazolyl spacer with an angle of about 90° (**15**; Fig. 13a), in order to favour cyclic arrangements.^{118,119} The authors accomplished model optimizations which suggested that the UPy subunits in **15** can adopt several defined conformations, each of them giving rise to cyclic oligomers of various sizes and shapes (Fig. 13a). On one hand, they discovered that a flat trimer or tetramer cannot be built due to torsional and steric reasons. However, when the UPy subunits in each monomer are pointing to opposite sides, folded structures can easily be arranged, leading to cyclic trimers or tetramers with propeller-like shapes (Fig. 13b). On the contrary, when both UPy subunits arrange in a mirror image relationship, pointing to the same side of the carbazole spacer, a very favourable, sterically unhindered tubular (belt-like) shape can be generated (Fig. 13b,c).

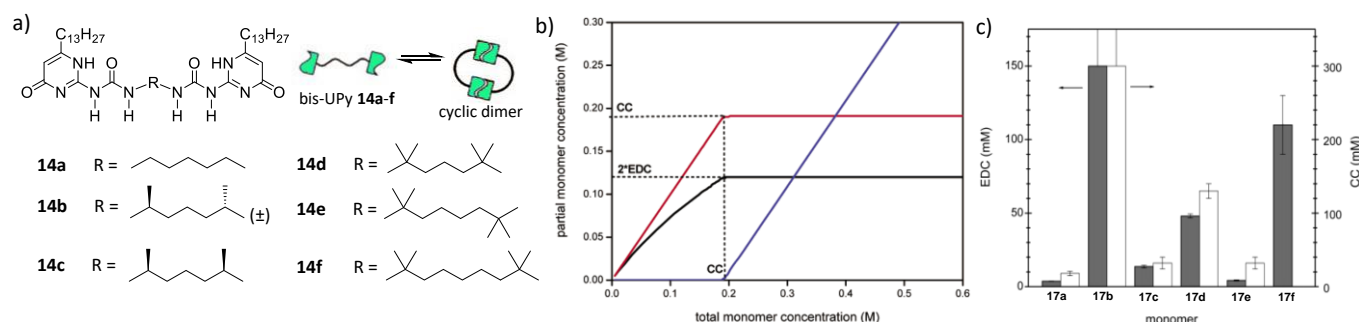


Fig. 12. (a) Structure of UPy derivatives **14a-f**. (b) Partial concentrations of linear polymers (blue), cyclic dimers (black), and the total of all cyclic assemblies (red), calculated for a 30 hypothetical system of equilibrating UPy assemblies. (c) Equilibrium cyclic dimer concentrations (EDC, gray, left axis) and critical concentrations (CC, white, right axis) in CDCl_3 solution, as determined by ^1H NMR analysis. Adapted with permission from ref. 79 Copyright 2004, American Chemical Society. Reproduced with permission from ref. 80. Copyright 2005 American Chemical Society.

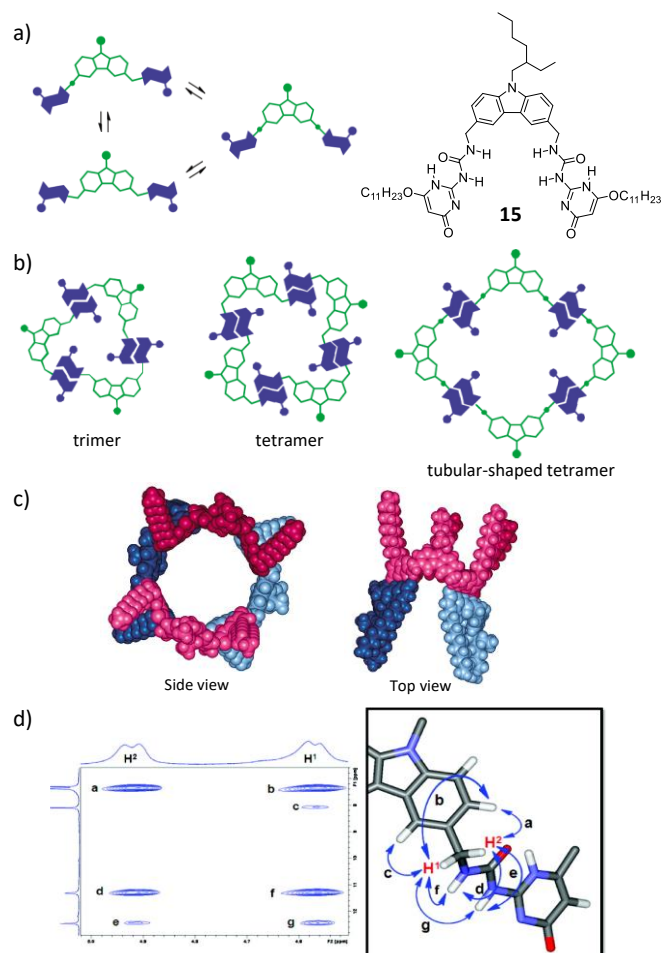


Fig. 13. (a) Disubstituted carbazole **15** and schematic representation of conformations around the UPy subunits. (b) Schematic representation of cyclic aggregates from **15**. (c) Side and top views of optimized tubular-shaped **c15₄** macrocycle. (d) Low-temperature (CDCl_3 , 213 K) NOESY spectrum of compound **15** (partial section showing contacts with methylene H^1 and H^2 protons). Adapted with permission from ref. 118. Copyright 2011 American Chemical Society.

As calculations predicted, the experimental work carried out by the group showed unequivocally that the tubular-shaped **c15₄** structure shown in Fig. 13c is the most abundant associated species. For instance, NMR experiments at 213 K (10 mM in CDCl_3) displayed a unique set of sharp signals for the UPy subunits, corresponding to a symmetric structure with a plane of symmetry bisecting the carbazole core. The methylene protons attached to the carbazoyl core split into two doublets, accounting for a rigid structure with different environments for each proton (Fig. 13d). The contacts observed in the NOESY (Nuclear Overhauser Effect Spectroscopy) experiments between H^1 and the 4-carbazoyl proton, and between H^2 and the 2-carbazoyl proton as well as with the urea protons, indicated that both H-bonded edges are oriented *anti* with respect to the

carbazoyl N -substituent (Fig. 13d), supporting the belt-shaped tetrameric geometry proposed.

A related example in which very specific conformational changes can regulate ring-chain equilibria was offered by Chen and co-workers. These authors used hydrazide-based supramolecular synthons linked through an isophthalamide spacer, with properly encoded recognition sites oriented in a 120° angle (compounds **16a-c**; Fig. 14a).

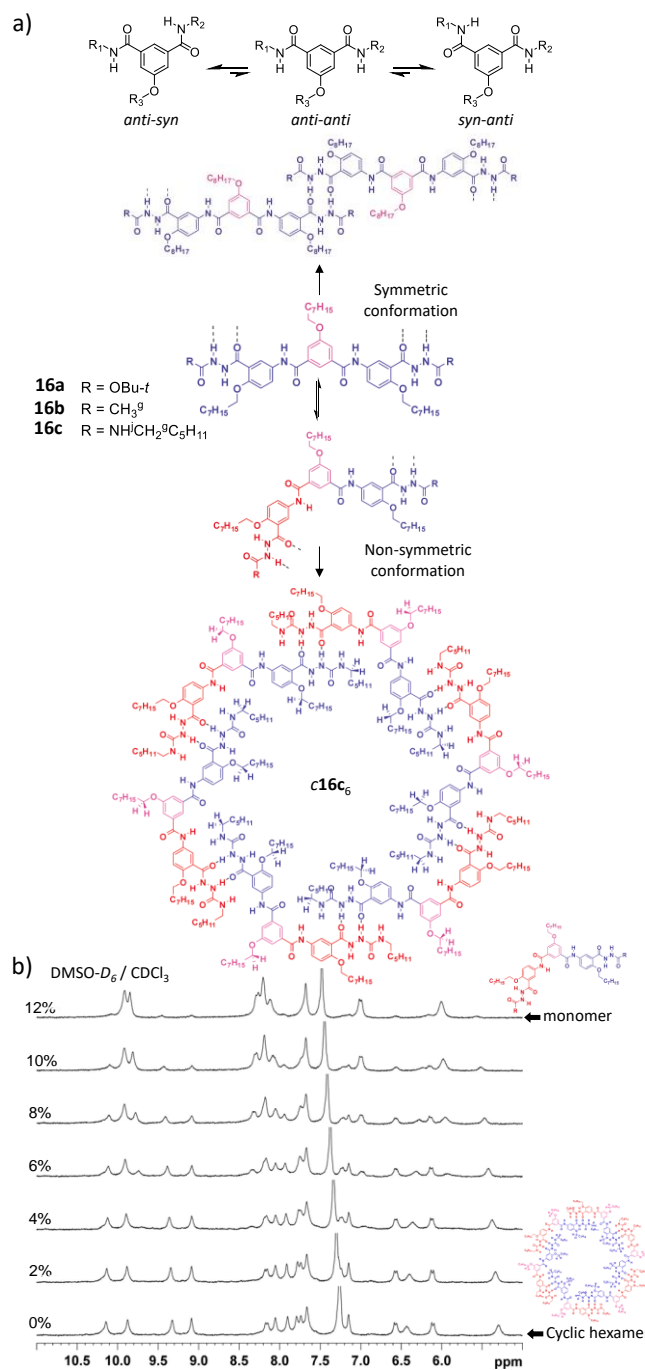


Fig. 14. (a) Chemical structure of ditopic monomers **16a-c** and representation of the association equilibrium of nonsymmetric vs symmetric conformations

of the 120° isophthalamide spacer into cyclic hexamer vs linear polymers, respectively. (b) ^1H NMR spectra of **16c** in CDCl_3 titrated with $\text{DMSO}-d_6$ (10 mM, 298 K, 300 MHz). Adapted with permission from ref. 120. Copyright 2009 American Chemical Society.

The conformational flexibility of the monomer allows for the generation of two main relative conformations of the recognition sites. As shown in Fig. 14a, a *syn-anti* or *anti-syn* non-symmetric conformation can lead to well-defined hexameric rosettes by double H-bonding between hydrazide fragments. In contrast, an *anti-anti* symmetric conformation would allow also the formation of linear polymers in solution,^{120,122} which may compete with the macrocyclization process. Dilution ^1H NMR experiments within a concentration range of 100–1 mM in CDCl_3 showed no prominent changes, suggesting the formation of cyclic supramolecular associates of **16a-c** (Fig. 14b). Besides, when a 10 mM solution of **16c** in CDCl_3 was titrated with $\text{DMSO}-d_6$, new signals corresponding to the monomer, in addition to the signals attributed to the hexamer, also appeared in slow exchange when the $\text{DMSO}-d_6$ content reached about 4%. No other signals associated with open species were found during the whole titration process (Fig. 14b). This observation, along with the high association constant calculated for the **c16c**₆ hexameric species (between *ca.* 10^{16} and 10^6 M^{-5} in CDCl_3 – $\text{DMSO}-d_6$ mixtures, in particular: $K_a = 3.67 \times 10^{16} \text{ M}^{-5}$ in 4% $\text{DMSO}-d_6/\text{CDCl}_3$), points to a highly cooperative “all-or-nothing” assembly process.

Interestingly, by changing the location of the alkoxy group in the central spacer of this kind of hydrazide-based monomers (from position 5 to position 4), the *syn-anti* non-symmetric conformation can be fixed (Fig. 15a) and, as a consequence, a highly regioselective noncovalent synthesis of the hydrazide-based cyclic hexamers was achieved. The authors observed that only one out of thirteen possible isomeric cyclic hexamers is selectively formed with precise control of the position of the two hydrazide units (*out* or *in*; Fig. 15a).¹²¹ ^1H NMR experiments of compounds **17a** and **17b** in CDCl_3 confirmed the formation of well-defined shape-persistent cyclic hexamers in solution, with a single set of signals for each part of the molecule (Fig. 15b). These results, together with the evidence of intermolecular contacts in the cyclic species observed by NOESY and COSY (*Correlation Spectroscopy*) NMR analysis, clearly show a precise control of the relative positions of the hydrazide units in the resulting cyclic hexamers, which underlines the high regioselectivity of this cyclization process.

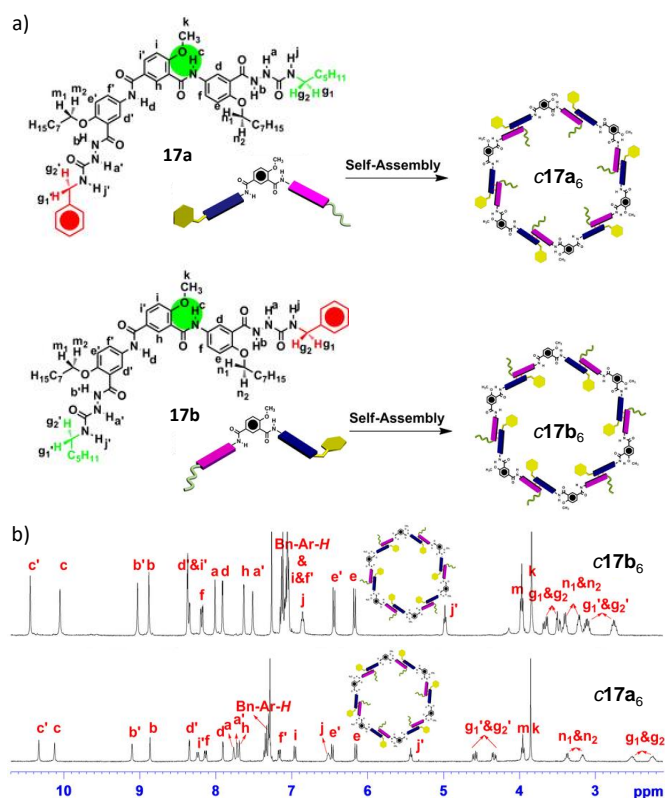


Fig. 15. (a) Regioselective self-assembly of compounds **17a-b**. (b) ^1H NMR spectra of cyclic hexamers **c17a₆** and **c17b₆** (CDCl_3 , 298 K, 10 mM). Adapted with permission from ref. 121. Copyright 2013 Nature Publishing Group.

The group of González-Rodríguez has recently established a versatile strategy to prepare H-bonded cyclic tetramers from dinucleoside monomers with a control on cycle size, shape and composition.^{122–125} A general monomer structure studied in the group comprises a π -conjugated *p*-diethynylbenzene unit substituted with complementary nucleobases at the edges (for example G and C bases, as in Fig. 16a). This rigid and linear linker structure, together with the 90° angle provided by Watson–Crick pairing, results in the formation of unstrained square-shaped H-bonded cyclic tetramers when the monomers adopt a *syn* conformation (*i.e.* the Watson–Crick edges point to the same side of the monomer). These cyclic species are in competition with linear oligomers, which may be formed by participation of *anti*-conformers (*i.e.* the Watson–Crick edges in the monomer point to opposite sides). These two main *syn* and *anti* conformations are both planar and maintain π -conjugation along the whole rigid monomer structure.

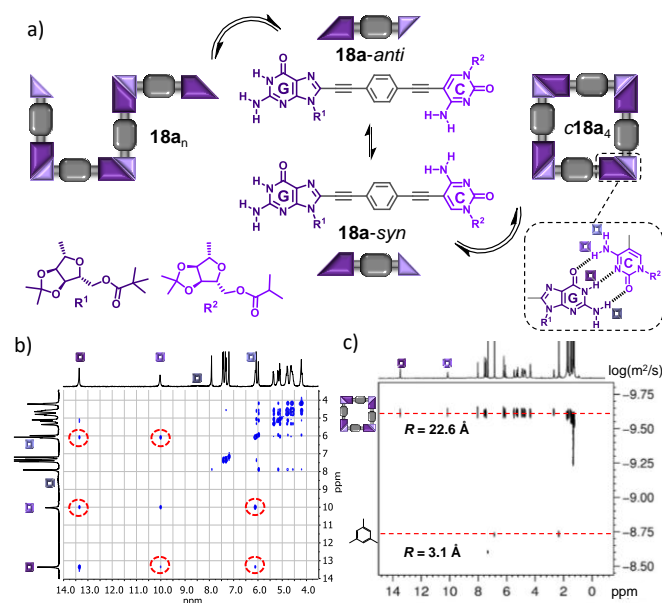


Fig. 16. (a) Conformational equilibrium and ring-chain supramolecular equilibrium established by G-C dinucleoside monomers like **18a**. (b) Downfield region of the NOESY NMR spectrum of **18a** in CDCl_3 at 298 K and 10^{-2} M, showing cross-peaks between the H-bonded G-amide and C-amine proton signals in the **c18a₄** macrocycle. (c) DOSY NMR spectrum of **18a** in CDCl_3 at 298 K and 10^{-2} M using mesitylene as internal reference. Adapted with permission from ref. 122. Copyright 2015 Wiley-VCH Verlag GmbH & Co. KGaA.

The self-assembly of this kind of dinucleoside monomers in solution was studied by different techniques and under diverse conditions. The group first analysed compound **18a**, comprising G and C nucleosides equipped with bulky lipophilic ribose groups (Fig. 16a), so as to afford solubility and prevent stacking interactions.¹²² It was demonstrated that a **c18a₄** cyclic tetramer structure was formed with high fidelity in organic solvents of low or moderate polarity, such as toluene, CHCl_3 or THF. ^1H NMR and NOESY experiments (Fig. 16b) confirmed G:C Watson-Crick pairing, while DOSY NMR revealed the presence of a single, well-defined associated species with a hydrodynamic radius that was consistent with a cyclic tetramer (Fig. 16c). Additionally, optical spectroscopy measurements at low concentrations showed that these cyclic species were characterized by red-shifted absorption and emission features and a Cotton CD (Circular Dichroism) effect (see Fig. 17d below).

All these spectroscopic characteristics were lost in conditions that favoured dissociation, such as low concentrations, high temperatures or solvents of increasing polarity. Interestingly, a strong “all-or-nothing” behaviour was observed, meaning that only a cyclic tetramer-monomer equilibrium (Fig. 17a) was monitored upon dissociation, and no other associated species (other cycles or open oligomers) were detected in the process. For instance, ^1H NMR dilution experiments in DMF-d_7 revealed an equilibrium between two species, **18a** and **c18a₄**, whose ^1H signals did not change in shape and position with temperature or concentration changes (Fig. 17b). Furthermore, these two species exchanged remarkably slowly ($k = 3.0 \pm 0.7 \text{ s}^{-1}$) in this polar solvent, as confirmed by EXSY (Exchange Spectroscopy) NMR experiments. The monomer-macrocycle equilibrium could

be also studied at lower concentrations in THF by absorption, emission and CD spectroscopy as a function of temperature or overall concentration (Fig. 17d).

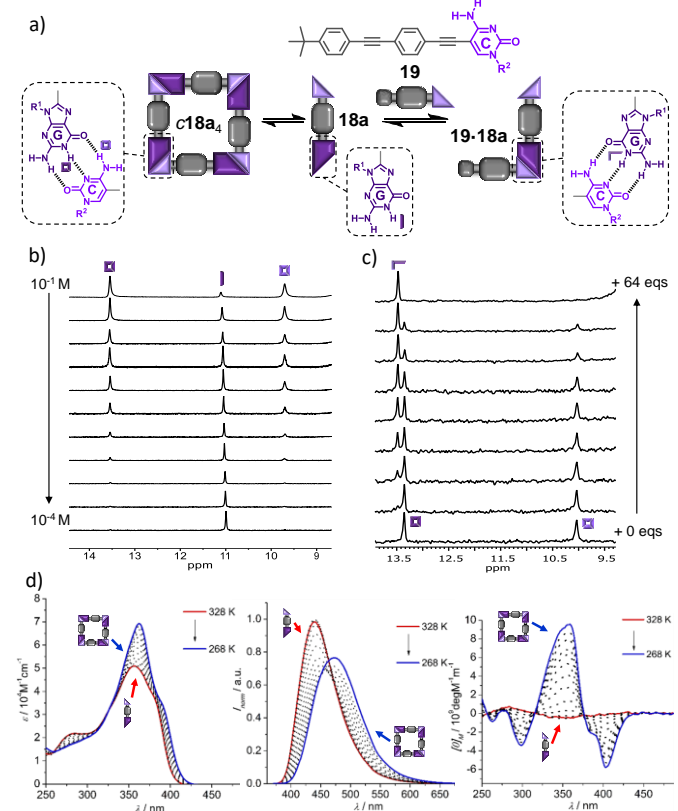


Fig. 17. (a) “All-or-nothing” monomer **18a** – **c18a₄** cyclic tetramer equilibrium. In the presence of an excess of mononucleoside competitor, like **19**, the equilibrium can be shifted to the C-GC **19-18a** bimolecular complex. Substituents R^1 and R^2 are shown in Fig. 16a. (b) Changes observed in the downfield region of the ^1H NMR spectra of **18a** in DMF-d_7 as a function of concentration at 298 K, showing the **18a**–**c18a₄** equilibrium in slow exchange. (c) ^1H NMR changes observed in the titration experiments of **18a** with increasing amounts of **19** in CDCl_3 at 298 K and constant 10^{-3} M **18a** concentration, showing the transition from **c18a₄** to **19-18a**. (d) from left to right: absorption, emission and CD changes of **18a** in THF as a function of temperature at 1.25×10^{-5} M, showing the **18a**–**c18a₄** transition. Adapted with permission from ref. 122. Copyright 2015 Wiley-VCH Verlag GmbH & Co. KGaA.

The high thermodynamic and kinetic stability displayed by these tetrameric macrocycles, was ascribed to the record chelate cooperativities attained ($EM = 10^2$ – 10^3 M) in solvents of very different nature, such as CHCl_3 , THF or DMF .²³ Such high cooperativities were confirmed through competition experiments in the presence of the corresponding mononucleoside compounds (like C derivative **19**; Fig. 17a). These kind of experiments represent an excellent method to evaluate chelate effects, since intra- and inter-molecular binding events are made to compete. In particular, it was shown that more than 50 equivalents of mononucleoside competitor **19** were required to fully break the **c18a₄** cyclic assemblies, by formation of the corresponding C-GC **19-18a** bimolecular complex (Figs. 17a and c).

Macrocycle Size. Contrary to unsaturated double or triple bonds, the presence of single σ -bonds in the linker connecting

the monomer binding sites allows for accessing several well-defined conformations that may lead to cyclic species, as the latter examples have demonstrated. Even if the binding sites are correctly arranged through rigid spacers to generate cyclic structures devoid of strain, the presence of these σ -bonds allow the monomer and associated species access to multiple conformations and degrees of freedom through rotational and torsional motions that are usually reduced upon cyclization. It is clear then that the higher the number of these single bonds in monomers of increasing length, designed to yield cycles of increasing size, should have a negative impact on the chelate cooperativity of the macrocyclization process.³⁸

The relationship between macrocycle size (or monomer length) and chelate cooperativity has been studied very recently in the group of González-Rodríguez, using the same kind of G-C dinucleoside monomers where the nucleobases are connected through π -conjugated linear spacers. On the basis of the previous described results, the researchers asked themselves how large they could build their cyclic tetramer assemblies.¹²⁶ To address this question they prepared a series of monomers in which the G and C terminal bases are separated by rigid oligo(phenylene-ethynylene) spacers of different lengths ($n = 1$ to 5; **18a–18e** in Fig. 18a), which resulted in H-bonded macrocycles of diverse diameters (3.6–7.4 nm). NMR and optical spectroscopic studies demonstrated that, as the length of the π -conjugated block increases, the macrocycles suffer a dramatic decrease in stability. Since the binding interaction is identical for all monomers (*i.e.* G:C Watson-Crick pairing), such destabilization was ascribed to a gradual and notable decrease in the *EM* of the system as the monomer length increases. This was for instance qualitatively observed in ^1H NMR titrations increasing the DMSO content in CDCl_3 -DMSO- d_6 mixtures (Fig. 18b). Firstly, contrary to a single G:C binding interaction (illustrated with a 1:1 mixture of G and C reference mononucleosides), which shows a fast exchange between bound and unbound species, the **c18a₄**–**c18e₄** macrocycles are always seen in slow exchange in the NMR timescale. Secondly, their resistance to DMSO decreases with the length of the spacer: **18a** > **18b** > **18c** > **18d** \approx **18e**. Finally, the dissociation of the larger **c18d₄**/**c18e₄** assemblies produced associated species that are in fast exchange with the monomer. This was attributed to the coexistence of short open oligomers (dimers, trimers) at low DMSO contents, and is a consequence of the loss of the “all-or-none” features observed for **c18a₄**–**c18c₄**, which was ascribed to a reduced chelate cooperativity in the larger assemblies.

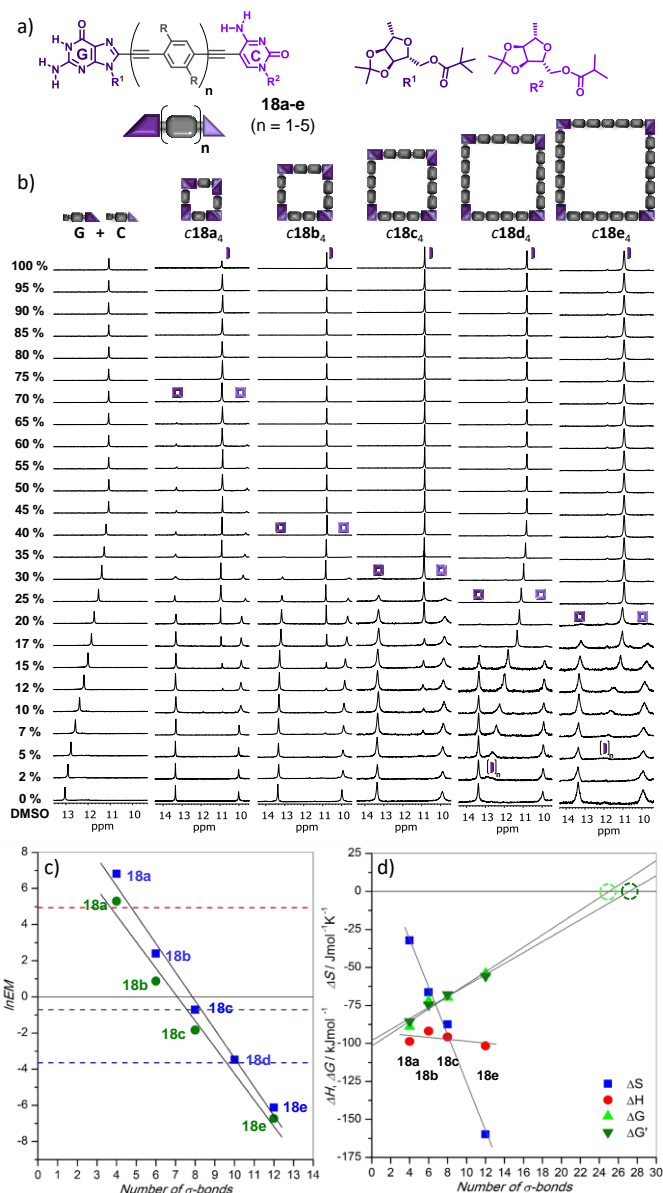


Fig. 18. Relationship between monomer length, macrocycle size and chelate cooperativity. (a) General structure of oligo(phenylene-ethynylene)-bridged G-C monomers **18a-e**, where $n = 1-5$. (b) Downfield region of the ^1H NMR spectra, showing the H-bonded G-amide (violet) and C-amine (light violet) proton signals, of a 1:1 mixture of reference G and C mononucleosides, and of **18a-e** dinucleosides as the volume fraction of DMSO- d_6 is increased in CDCl_3 -DMSO- d_6 mixtures at constant $1.0 \cdot 10^{-2}$ M concentration and 298 K. (c) Plots of $\ln EM$ vs number of σ -bonds for **18a-e** in THF (green circles) and CHCl_3 (blue squares). (d) Plot of ΔH , ΔG and ΔS values for cyclotetramerization vs number of σ -bonds for **18a-e** in THF and extrapolation to $\Delta G = 0$. Reproduced with permission from ref. 126. Copyright 2017 Wiley-VCH Verlag GmbH & Co. KGaA.

The five cycle sizes were analysed in three different solvent systems: DMF, THF and CHCl_3 , by means of diverse techniques. While these solvents had an expected, profound influence on the association constants between complementary nucleobases, the *EM* values did not show a clear solvent-dependence, and its natural logarithm showed a similar linear trend with the number of σ -bonds in the spacer in both CHCl_3 and THF (Fig. 18c). In addition, by building the corresponding

van't Hoff plots, the authors demonstrated that this reduction in *EM* is exclusively due to entropic reasons (Fig. 18d), presumably associated with the increasing loss of rotational and torsional degrees of freedom upon cyclotetramerization as the number of σ -bonds in the oligomeric spacer increases from 4 ($n = 1$) to 12 ($n = 5$). The extrapolation of the experimental trends obtained allowed the researchers to predict the maximum monomer lengths up to which the cyclic species can be assembled in competition with linear oligomers.

Extended π -conjugation. In subsequent work, the authors also studied biphenylene-bridged monomers, such as **20a** and **20b** (Fig. 19a).¹²⁹ These molecules were prepared with the aim to partially (**20a**) or totally (**20b**) block rotation around the central Csp^2 - Csp^2 σ -bond due to steric effects, as it is well-known in biphenylene chemistry,^{127,128} and therefore to investigate the influence of blocked rotors and internal π -conjugation on chelate cooperativity.

When examining solutions of different DMSO content in $CDCl_3$ at constant concentration by 1H NMR (Fig. 19b), clear differences in the self-assembly behaviour of **20a/b** were noted by the authors. Dinucleoside **20a** was able to self-assemble in cyclic tetramer species, showing slow exchange with the monomer and just slightly lower stabilities than the analogue molecule having an ethynylene unit connecting the two central phenylene rings (**18b**), since it could resist lower DMSO contents until full dissociation (35% vs 45%, respectively). In contrast, **20b** formed viscous solutions that exhibited much broader H-bonded signals that, upon addition of $DMSO-d_6$, revealed a gradual upfield shift, which is characteristic of open oligomers and reminiscent of the behaviour of a 1:1 mixture of G and C. The authors ascribed this qualitatively different self-assembly behaviour to the preferences for π -conjugation pathways in the monomers. Whereas **20a** can still adopt quasi-planar *syn*-type conformations that maintain both nucleobases in the same plane and that can therefore lead to cyclic assemblies, for **20b** this is severely hindered. Theoretical calculations revealed that **20b** prefers to adopt conformations in which each phenylene-ethynylene fragment is π -conjugated with the adjacent nucleobase ring (*Conformation II* in Fig. 19c). This conformation disposes the complementary nucleobases in orthogonal planes, which inhibits cyclotetramerization and instead favours supramolecular polymerization.

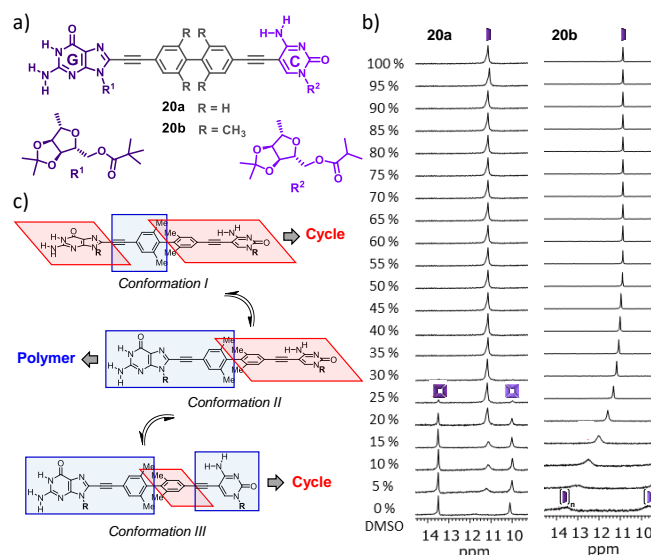


Fig. 19. (a) Scheme of the structure of biphenylene-bridged G-C monomers **20a-b**. (b) Downfield region of the 1H NMR spectra of **20a-b** dinucleosides as the volume fraction of $DMSO-d_6$ is increased in $CDCl_3$ - $DMSO-d_6$ mixtures at constant $1.0 \cdot 10^{-2}$ M concentration and 298 K. (c) Possible π -conjugated conformations adopted by **20b**, obtained by 90° rotation around the Csp^2 - Csp^2 σ -bonds. Blue and red planes are orthogonal to each other. Conformations I and III maintain the two bases in the same plane, and might thus lead to the formation of cyclic tetramers. However, in conformation II the two bases are in orthogonal planes and Watson-Crick pairing can only lead to open supramolecular polymers. Adapted with permission from ref. 129. Copyright 2018 Wiley-VCH Verlag GmbH & Co. KGaA.

Intramolecular Interactions

Intramolecular H-bonding. In view of the previous results, the group reasoned that shorter monomers than **18a**, having a lower number of σ -bonds connecting the complementary nucleobases, may produce even more stable cyclic assemblies. However, decreasing the space between H-bonding directors might also bring new effects related to steric hindrance between nucleobase substituents or intramolecular H-bonding interactions that can influence conformational equilibria at the monomer level, and therefore affect chelate cooperativities.

The ethynylene-bridged monomers (**21a-21d**; Fig. 20a) were synthesized with the purpose to investigate this issue.¹²⁹ The group soon realized that compounds **21a** or **21b**, having a bulky ribose group at the G nucleobase were not able to cyclize, and instead formed open supramolecular polymers that led to precipitation or solvent gelation (Fig. 20b). In contrast, replacing such G-ribose substituents by linear alkyl chains, as in **21c** or **21d**, allowed the cyclotetramerization process to take place. Computational calculations helped to understand the large differences in the self-assembly of these shortly spaced monomers. The presence of steric hindrance or electronic effects in the *syn* or *anti* conformers of **21a** or **21b** was ruled out, but an inspection of the optimized structures revealed the existence of H-bonding interactions between the C-amino group and the different oxygen atoms in the G-ribose moiety in the *anti* conformation (Fig. 20c). Such intramolecular H-bonding interactions significantly influence the *syn-anti* conformational preferences, blocking the structures in a spatial configuration

that is unfavourable for cyclization but favourable for polymerization.

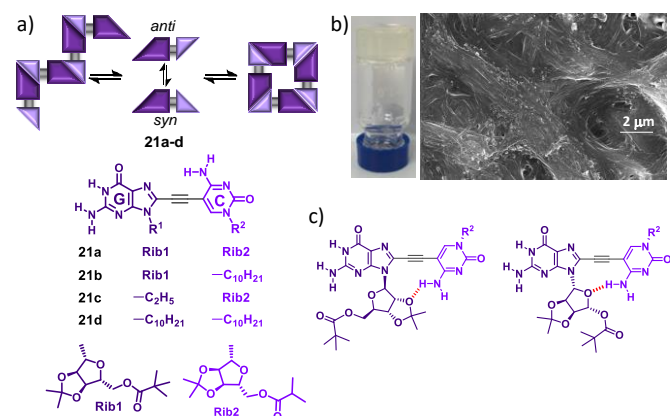


Fig. 20. (a) Ring-chain equilibrium in short, ethynylene-bridged G-C monomers **21a-d**, having either lipophilic ribose groups or linear alkyl chains as R^1 and R^2 substituents in the nucleobases. (b) Inverted vial pictures and SEM images of **21a** in chlorobenzene. (c) Possible intramolecular H-bonds patterns in **21a/21b** that can stabilize the *anti* conformer, where the Watson-Crick edges point to opposite directions and G:C association would lead to open supramolecular polymers. Adapted with permission from ref. 129. Copyright 2018 Wiley-VCH Verlag GmbH & Co. KGaA.

Intramolecular π - π stacking. By using the UPy scaffold, Wang and co-workers^{130,131} demonstrated the stabilization of cyclic species by intramolecular π - π stacking interactions. The authors reported a concentration-dependent ring-opening polymerization process of bifunctional UPy compounds bridged by 1,5-dioxynaphthalene (DNP) and oligo(ethyleneglycol) chains with different lengths (Fig. 21a). The ring-chain equilibria of monomers **22a-c** were investigated by a combination of diverse techniques, such as ^1H NMR, DOSY, single-crystal X-ray diffraction and viscometry. The experimental results demonstrated that, along with the quadruple H-bonding, an additional intramolecular π - π stacking interaction between the DNP group and the dimerized UPy motif in its cyclic form is taking place, and the strength of this π - π stacking interaction directly depends on the length of the oligo(ethyleneglycol) chain. Furthermore, the strong intramolecular π - π stacking interactions led to a great increase in the critical concentration for polymerization, stemming from an increased cycle stability (Fig. 21b). In fact, DOSY experiments (Fig. 21c) showed that monomer **22a**, with the shortest oligo(ethyleneglycol) chain, self-assembles exclusively as cyclic species over a broad concentration range (1.6–500 mM). However, the CPC values of monomer **22b** and **22c**, with longer oligoEO chains, are *ca.* 70 and 23 mM, respectively. As a result, a mixture of cyclic/open species can be observed. Further experiments showed that with the addition of cyclobis(paraquat-*p*-phenylene) cyclophane ring (CBPQT⁴⁺; Fig. 21b), a dynamic donor-acceptor [2]catenane, interlocked by quadruple H-bonding interactions over the entire concentration range, can be selectively obtained. This example provides an unconventional supramolecular strategy to control ring-chain equilibrium.

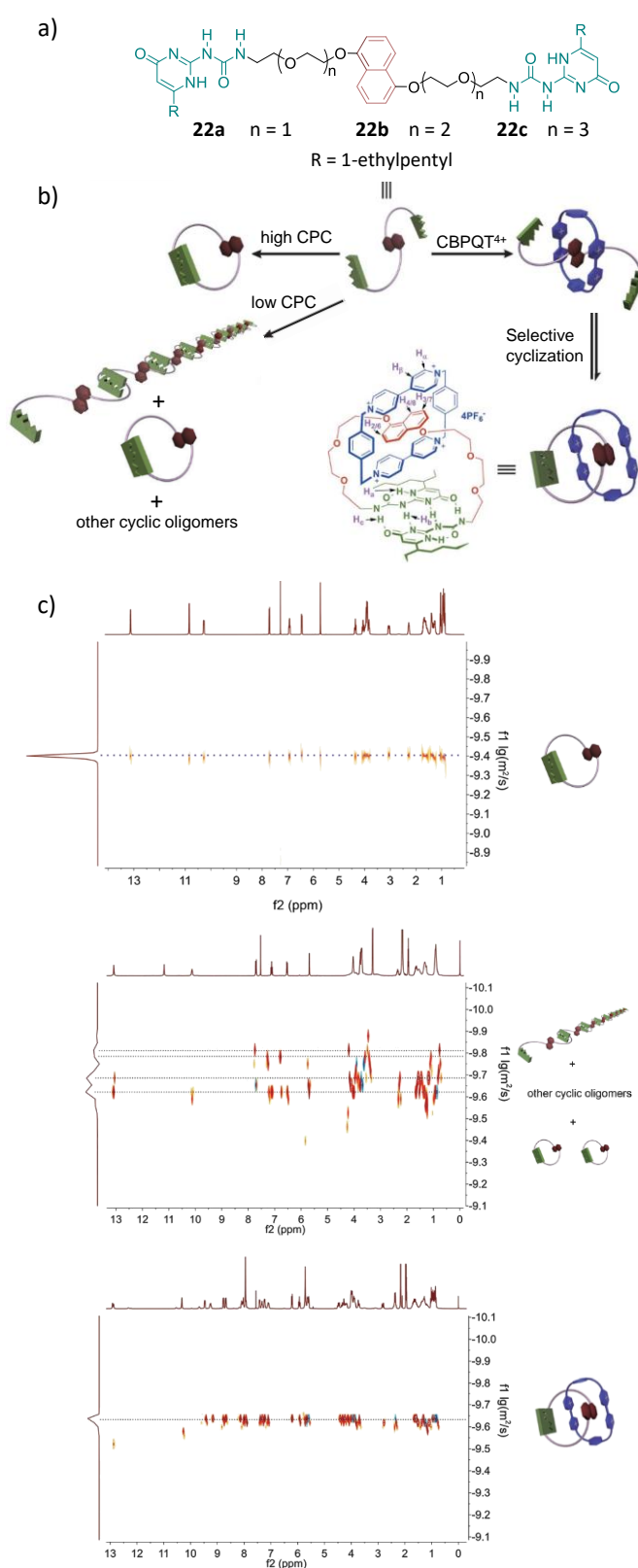


Fig. 21. (a) Monomers **22a-c** based on ureidopyrimidinone. (b) Graphical representation of the self-assembly behaviour of monomers **22a-c** in solution. (c) DOSY spectra of **22a** (top, 400 MHz, CDCl_3 , 298 K), **22b** (middle) and **22b-CBPQT⁴⁺** (bottom), (500 MHz, $\text{CDCl}_3/\text{CD}_3\text{CN}$ = 1/1, v/v, 293 K) and their proposed associated states at 200 mM. Adapted with permission from ref. 130 and ref. 131. Copyright 2012 Royal Society of Chemistry and American Chemical Society, respectively.

H-bonding Pattern

It is clear from all the studies highlighted so far in this article that the structure of the spacer connecting the two binding sites has a pronounced impact on the chelate cooperativity of the cyclization process and on the size of the self-assembled macrocycle attained. In fact, the nature and geometry of such a spacer are responsible for the flexibility/rigidity and topology of the monomer structure. However, the (usually multiple) H-bonding interactions used to construct these self-assembled macrocycles are highly directional and present a preferred binding geometry, which additionally contributes to define the cycle size with lowest strain but also, interestingly, can have a strong impact on the magnitude of *EM* upon cyclization, as will be demonstrated below.

Tautomers. If several tautomers can be formed in a given heterocyclic unit, diverse H-bonding patterns are obtained that may show different selectivity for cyclization or for binding to other complementary units. A classic example is represented by the UPy motif, that may alternate between tautomers with *DDAA* and *ADDA* H-bonding patterns, depending if this unit self-dimerizes or form heterocomplexes with 1,8-naphthyridine (NAPY) derivatives, respectively.^{132,133}

Phthalhydrazides are an interesting motif used as a module for obtaining stable supramolecular cyclic assemblies. These derivatives exist as an equilibrium of three tautomeric forms: lactim-lactam, lactam-lactam and lactim-lactim (Fig. 22a). Upon cyclotrimerization (Fig. 22b), the lactim-lactam, with two different H-bonding interfaces (*AD* and *A'D'*) becomes the preferred tautomer, presumably because of the repulsion in the other two tautomers involving adjacent nitrogen atoms of the same hybridization type. In this way, monomer **23** is able to self-assemble into trimeric disks of high stability in toluene *via* *DA-A'D'* H-bonding interactions, as temperature-dependent ¹H NMR and SEC (*Size Exclusion Chromatography*) experiments confirmed. Using suitable substituents, Zimmerman and his group also proved that these phthalhydrazide-based trimers can act as a powerful self-organizing unit and produce stacked triplets that form thermotropic columnar liquid crystals.¹³⁴

Isocytosine is another interesting heterocyclic unit that can alternate between the *N*¹-H tautomer, with a *DAA* H-bonding pattern, and the *N*³-H tautomer, offering instead a *DDA* pattern. These two tautomers can associate by complementary triple H-bonding interactions to form isocytosine dimers in apolar solvents.¹³⁵ Butkus, Wärnmarkt *et al.* profited from this fact to study the tautoleptic association of an enantiomerically pure curve-shaped monomer derived from bicycle[3.3.1]nonane, and flanked at both edges by isocytosine units (**24** in Fig. 23).¹¹¹ Supramolecular belt-like *c24*₄ tetrameric assemblies were obtained with high fidelity, as demonstrated by VPO, DOSY and GPC experiments. Interestingly, only the homoleptic H-bonded cyclic complex, comprising a single *C*₁-symmetric tautomeric form that combines *N*¹-H and *N*³-H isocytosines at the edges, was detected in solution. No sign for the formation of heteroleptic complexes, which would be assembled from two different isomers in which both isocytosines present the same *N*¹-H or *N*³-H tautomer, was obtained. Both belt structures,

homoleptic or heteroleptic, would be associated *via* triple *DAA-ADD* H-bonding interactions and should therefore present similar enthalpic gain, although it is clear from this study that **24** has a strong preference for cyclotetramerization as a single entity.

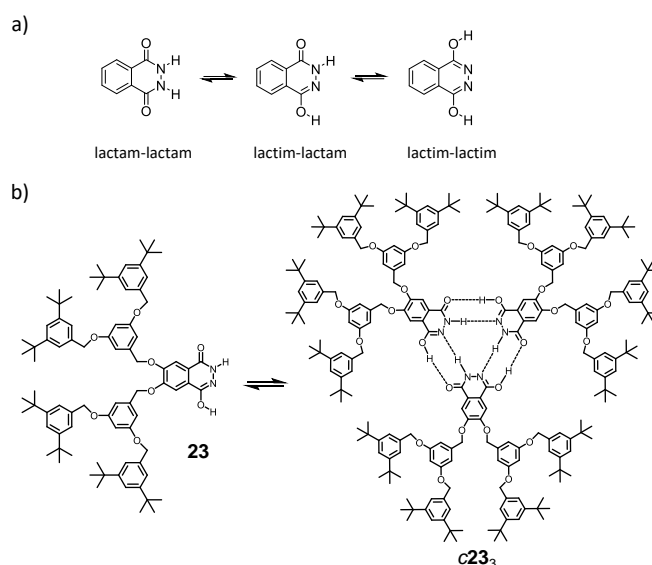


Fig. 22. (a) Phthalhydrazide tautomerization. (b) Self-assembly of the phthalhydrazide lactim-lactam cyclic trimer of monomer **23**.

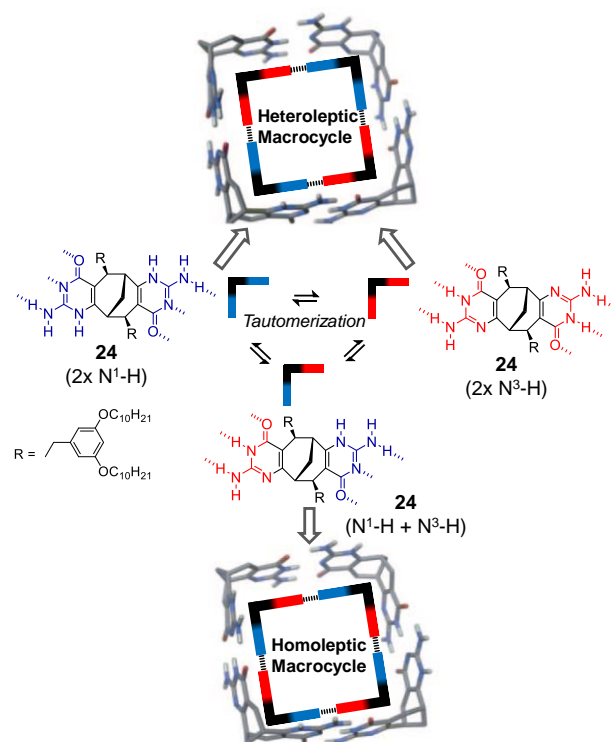


Fig. 23. Different *N*¹-H/*N*³-H isomers of monomer **24** obtained by tautomerization of the terminal isocytosines. Triple H-bonding between complementary faces can lead to either heteroleptic belt-like tetrameric cycles, combining two different tautomers, or homoleptic cycles, comprising a single tautomer with complementary edges. Adapted with permission from ref. 111. Copyright 2011 Wiley-VCH Verlag GmbH & Co. KGaA.

Symmetric (DAD-ADA) vs Unsymmetric (AAD-DDA/ADD-DAA) H-bonding Patterns. The group of González-Rodríguez has published a detailed study about the role of the symmetry of triple H-bonding interactions on the macrocyclization processes in solution¹²⁴ and on surfaces.¹³⁶ The authors compared the self-assembly of three related dinucleoside monomers,¹²⁴ comprising a rigid *p*-diethynylbenzene central block substituted at both edges with the corresponding complementary lipophilic nucleobases (G:C (**18a**), iG:iC (**25**), and 2-aminoadenine (aA)-U (**26**)),^{137,138} into their corresponding cyclic tetramers (Fig. 24a). 1D and 2D NMR experiments along with spectroscopic measurements like absorption, emission and CD, demonstrated that the **c18a₄** and **c25₄** cyclic tetramers exhibit comparably high thermodynamic stability and constitute kinetically steady products in the overall self-assembly landscape even in highly polar solvents like DMF, where H-bonded association is typically too weak.²³ However the aA-U monomer **26** associated in much weaker assemblies. This is already noted in concentration- and temperature-dependent experiments in CDCl₃ (Fig. 24b). Whereas the stronger G:C- and iG:iC-bound **c18a₄** and **c25₄** cyclic systems persist even at low concentrations and high temperatures, the aA:U-bound system displays two sets of proton resonances in slow exchange in CDCl₃. Upon dilution, the downfield shifted U-imide proton does not change in shape and position and is assigned to the cyclic **c26₄** species. The other U-imide proton signal grows in intensity at the expense of the former one and, importantly, is shifted upfield at low concentrations, suggesting the presence of a mixture of fast-exchanging, short, open oligomers (dimers, trimers,...) in equilibrium with the monomer. These experiments clearly reveal that the aA-U **c26₄** tetramer is not only weaker, but also loses the characteristic *all-or-nothing* cooperative behaviour noted for **c18a₄** (*vide supra*).

However, among all the measurements performed in different conditions, the competition experiments were

particularly revealing. In these, as explained above, the corresponding complementary mononucleoside competitor (**19/27/28**, see Fig. 24c,d) was gradually added to a solution of the associated tetramers (**c18a₄/c25₄/c26₄**) and the titration processes were monitored in solvents of low polarity by two different techniques: ¹H NMR spectroscopy at high concentrations (*ca.* 10⁻² M) and emission spectroscopy at relatively low concentrations (*ca.* 10⁻⁴ M). The results showed that whereas **c18a₄/c25₄** can resist up to 60 equivalents of the C-**19/iC-27** competitor, **c26₄** was fully dissociated after the addition of about 3 equivalents of U-**28**, regardless of the solvent system employed (Fig. 24e). These and other experiments afforded *EM* values for **c18a₄/c25₄** in the order of 10²–10³ M, while the **c26₄** cycle exhibited much lower chelate cooperativities (*EM* = 0.1–1 M). In other words, the symmetric DAD-ADA H-bonding pattern (aA:U), besides affording lower Watson-Crick association constants, explained by the unfavourable secondary H-bonding interactions according to the Jorgenssen model,⁵⁴ also provide weaker chelate effects than unsymmetric ADD-DAA (G:C) or DDA-AAD (iG:iC) patterns.

In order to explain these experimental results, the authors suggested (Fig. 25a) that the strong, unsymmetric ADD-DAA/DDA-AAD Watson-Crick H-bonding pattern directs binding with a 90° angle, which is the one required for cyclization. In contrast, the symmetric DAD-ADA H-bonding pattern, widely used to construct cyclic rosette structures,^{46-48,139-142} has also the possibility to associate *via* reverse Watson-Crick interactions, leading to a 210° angle, in addition to other double DA-AD H-bonding modes of comparable association strength. The presence of these multiple association modes in aA:U allows the linear oligomers to access a large number of binding possibilities and degrees of freedom that must be lost upon cyclotetramerization, which affects dramatically the *EM* of the system.

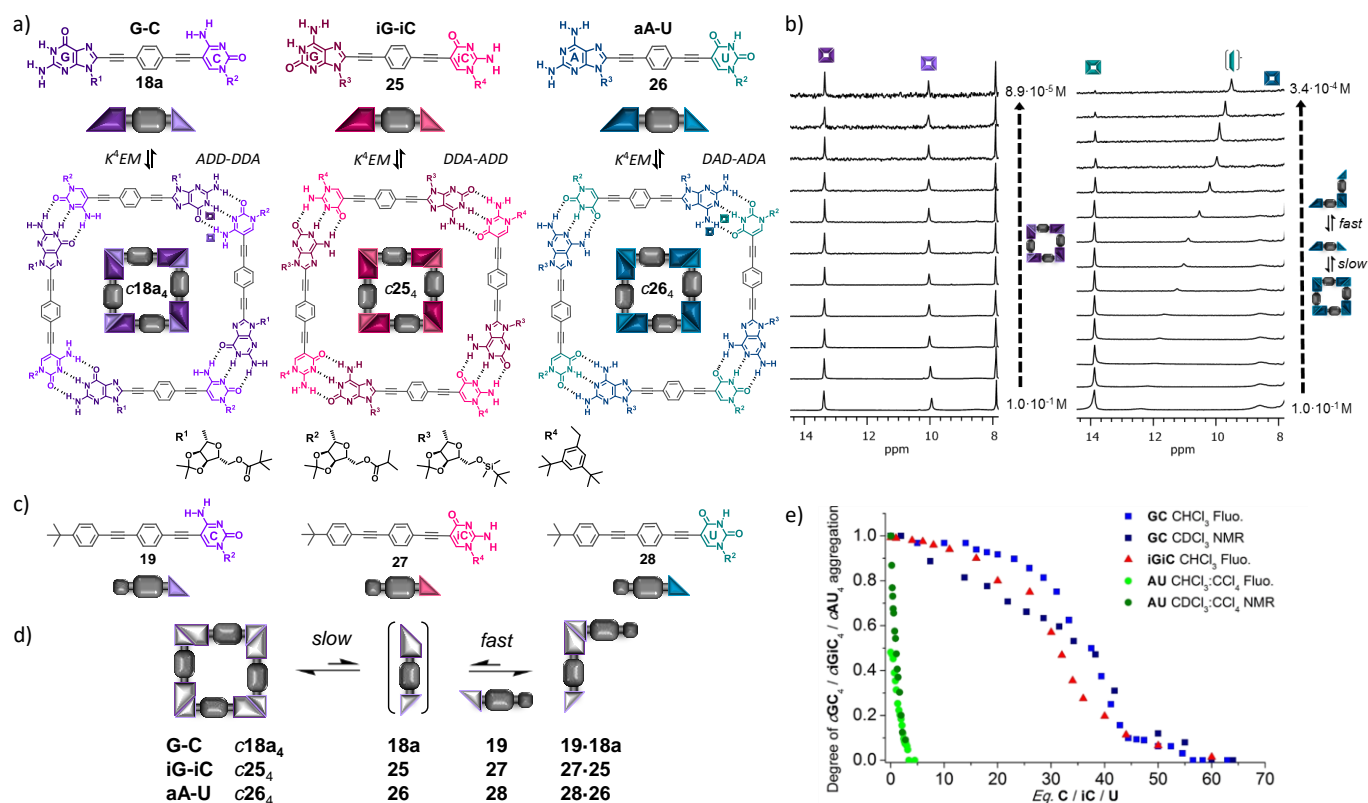


Fig. 24. (a) Chemical structure of G-C, iG-iC, and aA-U dinucleosidic monomers **18a**, **25** and **26** and their respective cyclic tetramers. (b) 14-8 ppm region of the ¹H NMR spectra of **18a** and **26** in CDCl₃ at different concentrations. (c) C, iC and U mononucleosides stoppers **19**, **27** and **28** used as competitors. (d) Competition experiments: plots of the degree of **c18a₄**, **c25₄** and **c26₄** association, as measured by either ¹H NMR or fluorescence spectroscopy, as a function of the equivalents of **19/27/28** respectively added (e). Adapted with permission from ref. 124. Copyright 2016 Wiley-VCH Verlag GmbH & Co. KGaA.

Collecting all available data of the association constants (K_a) between complementary pairs in CHCl₃, as well as the EM values derived from their work, the authors simulated the speciation profiles of the unsymmetric $ADD-DAA/DDA-AAD$ and symmetric $DAD-ADA$ H-bonded systems as a function of overall concentration (Fig. 25b). These simulations visually demonstrate that the use of an unsymmetric $ADD-DAA/DDA-AAD$ H-bonding pattern, providing moderate K_a and high EM values, leads to cyclic tetramer assemblies (**cM₄**) that persist as the main species in solution over a broad concentration range. For the weaker $DAD-ADA$ system, presenting both low K_a and EM values, the cyclic **cM₄** species is only predominant within a very narrow concentration window, and is in equilibrium with the monomer (**M**) and short open oligomers (**M_n**).¹²⁴ These two situations are clearly corroborated in the dilution experiments in CDCl₃ within the 10⁻¹-10⁻⁴ M regime shown in Fig. 24b. Finally, the authors also simulated a hypothetical symmetric $DDD-AAA$ system and compared it with the other two (Fig. 25b, bottom).

In this case, the $DDD-AAA$ pattern would lead to more strongly bound assemblies along the whole concentration scale, as a result of a high K_a value, although higher-order linear oligomers begin to compete strongly at moderate concentrations, since this symmetric pattern should enjoy lower EM values than the unsymmetric pattern.

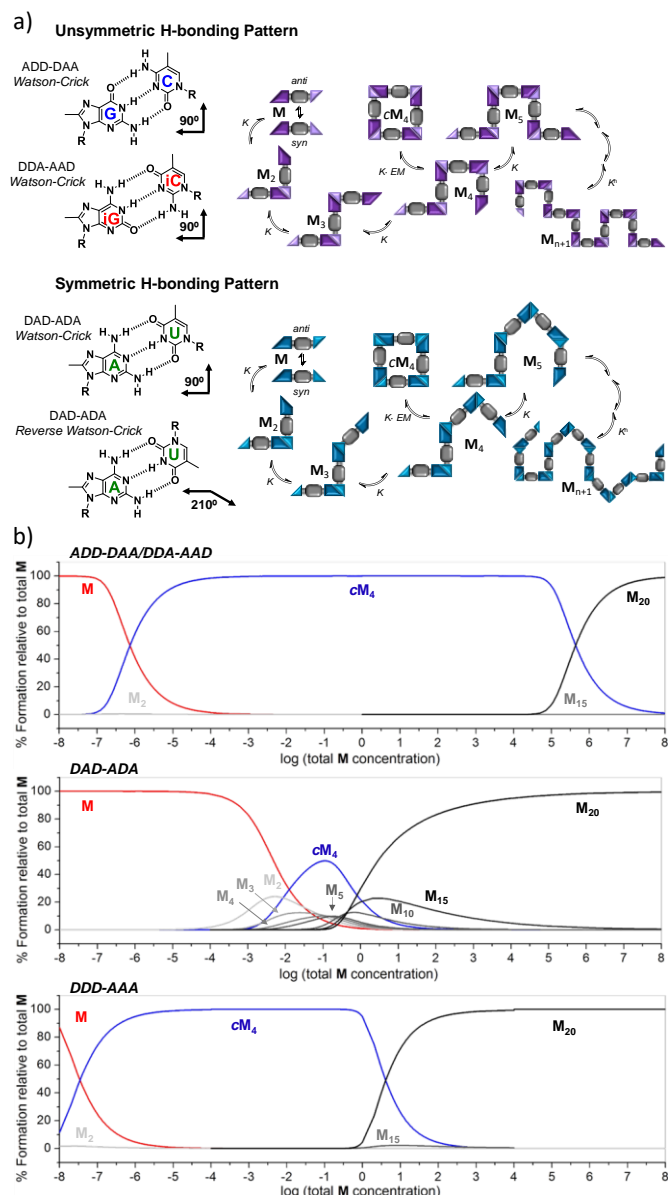


Fig. 25. (a) Ring-chain supramolecular equilibria in unsymmetric vs symmetric H-bonding patterns. (b) Simulated speciation curves for the H-bonded self-assembly of a hypothetical DDD-AAA ($K_{ref} = 10^6 \text{ M}^{-1}$; $EM = 0.05 \text{ M}$), ADD-DAA/DDA-AAD ($K_{ref} = 10^4 \text{ M}^{-1}$; $EM = 500 \text{ M}$) and DAD-ADA ($K_{ref} = 10^2 \text{ M}^{-1}$; $EM = 0.05 \text{ M}$) ditopic monomers. Reproduced with permission from ref. 124. Copyright 2016 Wiley-VCH Verlag GmbH & Co. KGaA.

The versatility of these general dinucleoside system allows for the introduction of any rigid central block between the bases, as long as it is linearly disubstituted. In a more recent work the same authors included FRET (*Förster Resonance Energy Transfer*) dye pairs (a benzodithiophene donor and a BODIPY acceptor) in mono-⁵⁹ and dinucleoside¹²⁵ systems, so as to study their association by fluorescence energy transfer measurements. Again, symmetric aA:U and unsymmetric G:C triple H-bonding patterns were compared, resulting in the same stability trends and related EM values as those obtained in their previous work. However, when analysing the chelate cooperativity of the corresponding cyclic tetramers by competition experiments with mononucleosides, the use of

complementary FRET dyes that absorb and emit in different spectral regions allowed the authors to monitor different supramolecular processes that other spectroscopic techniques failed to disclose. Specifically, when only a small excess of mononucleosides were added, these were able to bind strongly to the cyclic tetramers without actually causing their dissociation. The addition of a larger excess, however, ultimately led to cyclic tetramer dissociation and formation of the bimolecular complex between dinucleoside and mononucleoside, as observed by other techniques.¹²⁵

The DDD-AAA H-Bonding Pattern. Almost in the same period of time, the Severin lab published a work on the preparation of new and easily accessible polytopic building blocks for the construction of molecularly defined AAA-DDD cyclic nanostructures (Fig. 26a).¹⁴³ ITC (*Isothermal Titration Calorimetry*) experiments allowed the calculation of an association constant of $1.1 \cdot 10^7 \text{ M}^{-1}$ for the DDD-AAA **29:30** system in CHCl_3 , but no further experiments were possible owing to the fact that both compounds are non-fluorescent. By applying their synthetic procedure to aromatic dialdehydes, the authors were able to access the corresponding ditopic DDD-DDD (**31, 32**) and AAA-AAA (**33, 34**) units (Fig. 26b). These more complex systems showed a large degree of preorganization, promoting a macrocyclization process in two-component tetrameric systems. For instance, ^1H NMR experiments of equimolar amounts of **31** and **33** in CD_2Cl_2 revealed upfield shifts of the aromatic H-a and H-A signals as well as significant downfield shifts and broadening of the NH-B signals of **31**, which pointed to macrocycle formation (Fig. 26c). The analysis of these solutions by high-resolution mass spectrometry with nano-electrospray ionization gave a clean mass spectrum, with the two most prominent peaks corresponding to the ions $c[\mathbf{31}_2\mathbf{33}_2(\text{BArF})]^{3+}$ and $c[\mathbf{31}_2\mathbf{33}_2(\text{BArF})_2]^{2+}$ (Fig. 26d). DOSY experiments confirmed that the donor-acceptor combinations **31+33**, **31+34**, **32+33** and **32+34** exclusively gave the corresponding [2+2] macrocycles with different sizes (Fig 26b). All set of experiments carried out in this work allowed the authors to prove, for the first time, the formation of tetrameric macrocycles based on AAA-DDD interactions.

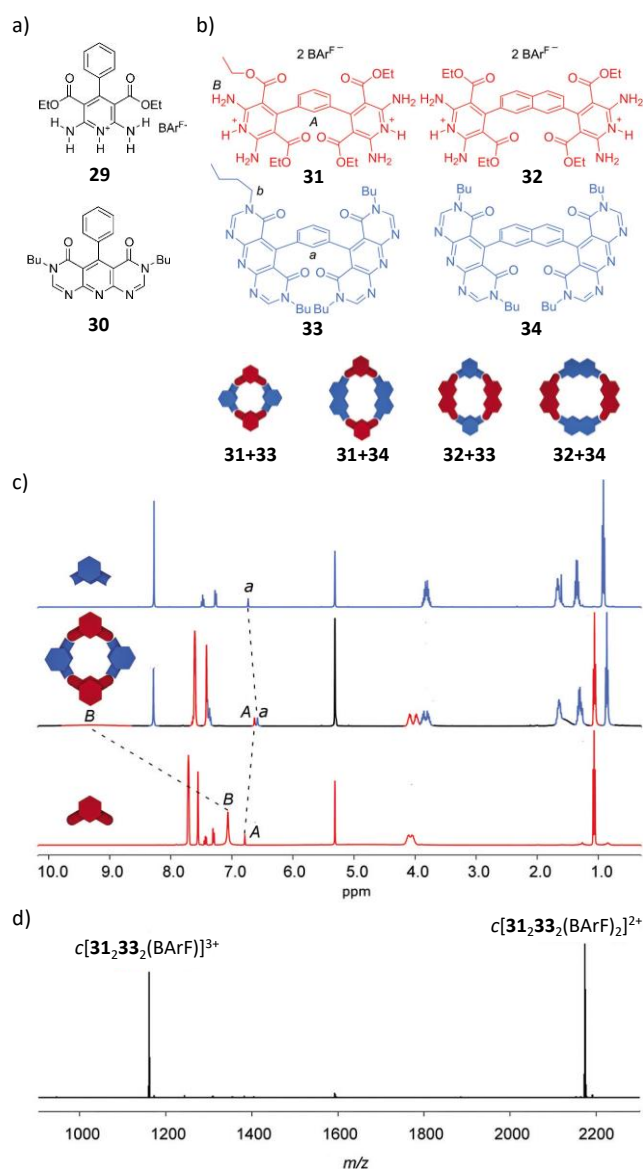


Fig. 26. (a) DDD (29 and AAA (30) building blocks. (b) Ditopic DDD-DDD (31, 32) and AAA-AAA (33, 34) building blocks and [2+2] macrocycles. (c) ¹H NMR spectra (CD₂Cl₂, 298 K, 400 MHz) of (top) donor 33, an equimolar mixture of 31 and 33 (center) and (bottom) acceptor 31. (d) ESI mass spectrum of a solution containing 31 and 33 showing peaks corresponding to the tetramer. Adapted with permission from ref. 143. Copyright 2016 Wiley-VCH Verlag GmbH & Co. KGaA.

Conclusions

In this Feature Article we have highlighted some selected examples from the literature that illustrate the effect of different parameters on the fidelity of H-bonding macrocyclizations of ditopic monomers.

In this scenario, we have seen along this review that such monomers can either “decide” to polymerize in open, linear species or, upon reaching a certain size, cyclize into discrete closed species. It is clear that entropic factors are in favour of intramolecular vs intermolecular binding interactions. For instance, if we consider a monomer (**M**) that has formed a linear tetramer (**M**₄) and now the system can either grow larger by

incorporation of another **M** molecule, leading to a linear pentamer (**M**₅), or the binding sites at the edges can interact intramolecularly leading to a cyclic tetramer (**cM**₄; please see Fig. 1). In the first case, two species condense into one, and several translational and rotational degrees of freedom are lost, which is entropically penalized. In the second case, the molecularity of the system remains unaltered, which benefits the intramolecular association, and hence cyclization.

Now, to evaluate how favourable is the cyclization process, one should compare open (**M**₄) and closed (**cM**₄) species. The latter is stabilized with respect to the former by the product *K-EM*, where *K* is the intermolecular association constant, because there is an additional binding interaction to close the cycle, and *EM* takes into account that this last binding event is not really intermolecular, but intramolecular. A qualitative evaluation of the expected magnitude of *EM* should then consider first the degrees of freedom that are lost upon cyclization. The molecule **M** may have several bonds that allow for some degree of conformational freedom by rotation and torsion, and some of these degrees may be lost when the cycle is formed, which is penalized by entropy. We have also shown that the binding interaction itself may play an important role as well. Some H-bonding moieties can have multiple association modes of comparable strength, which also introduces several degrees of freedom in the linear oligomers. In contrast, the formation of a particular cycle usually demands only one of these association modes. So, it is clear that, in order to enhance *EM*, both the monomer structure and the binding interaction should work optimally in concert. A clear conclusion obtained from this review is that rigid monomers with the lowest possible number of conformational possibilities, that arrange the binding sites in a particular geometry, and binding modes with a defined geometry, that are much stronger than any other possible binding mode, are obviously the right choice.

This analysis takes us to the concept of *preorganization* and the well-known fact that monomers that are correctly preorganized in a rigid structure lead to very stable closed assemblies. However, if such preorganization is not perfect, strain is generated in the cyclic structure, which is now penalized by the enthalpic term of *EM*. Hence, some degree of flexibility may be in some cases required to reach a particular cycle size. An improper preorganization for a particular cycle size may result in competition, not only with linear species, but also between several cycles of different molecularity, as disclosed in several examples found in the literature. In this situation, the use of templates that establish additional noncovalent bonds with a given cycle or the introduction of intra-cycle interactions that stabilize the desired ring and/or destabilize the non-desired competitors, may shift these equilibria.

In addition, all along this review article we have tried to highlight the different techniques, methods and strategies used by diverse authors to characterize the H-bonded structures, confirm their cyclic nature, and estimate their size.

First of all, intermolecular association into linear polymers usually leads to large aggregates that increase the viscosity of the medium, produce gels, or simply precipitate. Discrete cyclic

structures, in contrast, display high solubilities, especially if the macrocycles do not have a strong tendency to aggregate further by interaction, for instance, between peripheral H-bonding groups that are not occupied in ring closure.

^1H NMR experiments are without doubt the first choice to characterize H-bonded assemblies. Information about the symmetry of the ensemble and the protons that participate in H-bonding can be instantly obtained from the number of signals and their chemical shift, respectively. Very broad signals are detected for ill-defined open polymers, whereas cyclic structures often supply sharp signals that are not very sensitive to temperature, concentration and solvent composition changes. Variation of any of these three parameters may lead to dissociation, which is a useful way to determine the cyclic nature of the system. This is because a rather general attribute of cyclic structures is that they are kinetically more stable than open oligomers and often exchange slowly in the NMR timescale. Therefore, when they dissociate into non-cyclic or monomer species, two sets of signals are detected in slow exchange, which allows for the estimation of their relative concentration by ^1H NMR integration and for the calculation of diverse thermodynamic and kinetic parameters. Besides, as shown in several examples of this work, monitoring dissociation as a function of any of the above-mentioned parameters may also give a rough idea of the magnitude of the “all-or-none” cooperativity of the system under study. For instance, a very convenient way to evaluate macrocycle formation and compare relative cycle stabilities is to perform ^1H NMR experiments in which the volume fraction of a polar, competing solvent (like DMSO- d_6) is gradually increased in mixtures with an apolar solvent (like CDCl_3). Cycle dissociation monitored in this way may provide a qualitative indication for the formation of cyclic species and the magnitude of the chelate effect. Another way to induce dissociation and obtain qualitative and quantitative information about the cyclization process, as illustrated in this review, is to make intra- and intermolecular interactions compete by titration experiments with the corresponding monotopic molecule.

On the other hand, details about the arrangement of the molecular constituents, preferred conformations, or the H-bonding mode/tautomeric form in the cyclic assembly can be obtained from 2D NMR measurements, like NOESY/ROESY and COSY. In some cases, the fixation of a particular monomer conformation upon cycle formation may also bring about additional changes in absorption, emission or even CD (if the cycle can adopt a chiral arrangement) spectroscopies. Finally, several techniques may help in the determination of cycle size that are very different in nature and thus complementary. These include osmometry (VPO), chromatography (SEC/GPC), NMR (DOSY), or mass spectrometry techniques of different types (ESI-MS, for instance). Sometimes, comparing the fitting of experimental data to different cycle sizes may be also valuable to select the most probable assembly size.

In short, we hope the guidelines provided in this work will be useful for the future construction and study of novel supramolecular macrocyclic structures, not only monocyclic and H-bonded, but also polycyclic (cages, prisms, etc.) and

assembled by other noncovalent interactions. As a matter of fact, the factors influencing chelate cooperativity collected herein are common to any supramolecular process that leads to discrete, closed architectures. We also hope this work will help early-stage researchers to design, assess and characterize supramolecular cyclic structures, thus eventually contributing to a broader comprehension of chelate cooperativity and ring-chain equilibria.

Acknowledgements

Funding from MINECO (CTQ2017-84727-P) is gratefully acknowledged. F. A. acknowledges the European Union for financial support through a H2020-MSCA-COFUND-FP *Intertalentum* Fellowship.

Notes and references

- 1 H.-J. Schneider, *Angew. Chem. Int. Ed.*, 2009, **48**, 3924.
- 2 C. A. Hunter and H. L. Anderson, *Angew. Chem. Int. Ed.*, 2009, **48**, 7488.
- 3 G. Ercolani and L. Schiaffino, *Angew. Chem. Int. Ed.*, 2011, **50**, 1762.
- 4 L. K. S. von Krbek, C. A. Schalley and P. Thordarson, *Chem. Soc. Rev.*, 2017, **46**, 2622.
- 5 *Nat. Chem. Biol.*, 2008, **4**, 433.
- 6 A. Camara-Campos, D. Musumeci, C. A. Hunter and S. Turega, *J. Am. Chem. Soc.*, 2009, **131**, 18518.
- 7 C. A. Hunter, M. C. Misuraca and S. M. Turega, *J. Am. Chem. Soc.*, 2011, **133**, 582.
- 8 D. González-Rodríguez and A. P. H. J. Schenning, *Chem. Mater.*, 2011, **23**, 310.
- 9 A. P. H. J. Schenning and D. González-Rodríguez, in *Organic Nanomaterials: Synthesis, Characterization, and Device Applications*, John Wiley & Sons, Inc., Hoboken, New Jersey, 2015, p. 33.
- 10 S. Di Stefan, S. and G. Ercolani, Equilibrium Effective Molarity As a Key Concept in Ring-Chain Equilibria, Dynamic combinatorial Chemistry, Cooperativity and Self-assembly in *Advances in Physical Organic Chemistry*, Elsevier Ltd., 2016, Volume 50, Chapter 1, p. 1.
- 11 L. Yang, X. Tan, Z. Wang and X. Zhang, *Chem. Rev.*, 2015, **115**, 7196.
- 12 T. F. A. De Greef, M. M. J. Smulders, M. Wolffs, A. P. H. J. Schenning, R. P. Sijbesma and E. W. Meijer, *Chem. Rev.*, 2009, **109**, 5687.
- 13 M. I. Page and W. P. Jencks, *Proc. Nat. Acad. Sci. U.S.A.*, 1971, **68**, 1678.
- 14 M. I. Page, *Chem. Soc. Rev.*, 1973, **2**, 295.
- 15 C. A. Hunter, M. C. Misuraca and S. M. Turega, *J. Am. Chem. Soc.*, 2011, **133**, 20416.
- 16 M. D. Segarra-Maset and S. M. Turega, *J. Org. Chem.*, 2011, **76**, 2723.
- 17 C. A. Hunter, M. C. Misuraca and S. M. Turega, *Chem. Sci.*, 2012, **3**, 589.
- 18 C. A. Hunter, M. C. Misuraca and S. M. Turega, *Chem. Sci.*, 2012, **3**, 2462.
- 19 W. Jiang, K. Nowosinski, N. L. Löw, E. V. Dzyuba, F. Klautzsch, A. Schäfer, J. Huuskonen, K. Rissanen and C. A. Schalley, *J. Am. Chem. Soc.*, 2012, **134**, 1860.
- 20 H. Adams, E. Chekmeneva, C. A. Hunter, M. C. Misuraca, C. Navarro and S. M. Turega, *J. Am. Chem. Soc.*, 2013, **135**, 1853.
- 21 H. Sun, C. Navarro and C. A. Hunter, *Org. Biomol. Chem.*, 2015, **13**, 4981.

- 22 H. Sun, C. A. Hunter, C. Navarro and S. Turega, *J. Am. Chem. Soc.*, 2013, **135**, 13129.
- 23 P. Motloch and C. A. Hunter, Thermodynamic Effective Molarities for Supramolecular Complexes in *Advances in Physical Organic Chemistry*, Elsevier Ltd., 2016, Volume 50, Chapter 2, p. 77.
- 24 S. Henkel, M. C. Misuraca, Y. Ding, M. Guitet and C. A. Hunter, *J. Am. Chem. Soc.*, 2017, **139**, 6675.
- 25 L. K. S. von Krbek, A. J. Achazi, S. Schoder, M. Gaedke, T. Biberger, B. Paulus and C. A. Schalley, *Chem. Eur. J.*, 2017, **23**, 2877.
- 26 H. J. Hogben, J. K. Sprafke, M. Hoffmann, M. Pawlicki and H. L. Anderson, *J. Am. Chem. Soc.*, 2011, **133**, 20962.
- 27 S. Henkel, M. C. Misuraca, Y. Ding, M. Guitet and C. A. Hunter, *J. Am. Chem. Soc.*, 2017, 139, 6675.
- 28 M. J. Mayoral, N. Bilbao and D. González-Rodríguez, *ChemistryOpen*, 2016, **5**, 10.
- 29 F. Würthner, C.-C. You and C. R. Saha-Möller, *Chem. Soc. Rev.*, 2004, **33**, 133.
- 30 Fujita, M. Tominaga, A. Hori and B. Therrien, *Acc. Chem. Res.*, 2005, **38**, 369.
- 31 G. Guichard and I. Huc, *Chem. Commun.*, 2011, **47**, 5933.
- 32 R. Chakrabarty, P. S. Mukherjee and P. J. Stang, *Chem. Rev.*, 2011, **111**, 6810.
- 33 T. K. Ronson, S. Zarra, S. P. Black and J. R. Nitschke, *Chem. Commun.*, 2013, **49**, 2476.
- 34 T. R. Cook and P. J. Stang, *Chem. Rev.*, 2015, **115**, 7001.
- 35 G. Ercolani, *J. Phys. Chem. B*, 1998, **102**, 5699.
- 36 G. Ercolani, *J. Phys. Chem. B*, 2003, **107**, 5052.
- 37 G. Ercolani, in *Non-Covalent Multi-Porphyrin Assemblies*, ed. E. Alessio, Springer Berlin Heidelberg, Berlin, Heidelberg, 2006, p. 167.
- 38 S. Di Stefano and L. Mandolini, *Phys. Chem. Chem. Phys.*, 2019, **21**, 955.
- 39 A. J. Kirby, *Adv. Phys. Org. Chem.*, 1980, **17**, 183.
- 40 L. Mandolini, *Adv. Phys. Org. Chem.*, 1986, **22**, 1.
- 41 R. Cacciapaglia, S. Di Stefano and L. Mandolini, *Acc. Chem. Res.*, 2004, **37**, 113.
- 42 P. Ballester and J. de Mendoza, Supramolecular Macrocyclic Synthesis by H-bonding Assembly in *Modern Supramolecular Chemistry: Strategies for Macrocyclic Synthesis*; F. Diederich, P. J. Stang, R. R. Tykwinski, Eds.; Wiley VCH: Weinheim, 2008, p. 69.
- 43 P. Schuster, G. Zundel and C. Sandorfy, in *The Hydrogen bond: Recent developments in theory and experiments*. North-Holland Pub. Co., Amsterdam, 1976.
- 44 G. A. Jeffrey, in *An Introduction to Hydrogen Bonding*, Oxford University Press, New York and Oxford, 1997.
- 45 G.R. Desiraju, and T. Steiner, in *The Weak Hydrogen Bond*, Oxford University Press, Oxford, 1999.
- 46 B. Adhikari, X. Lin, M. Yamauchi, H. Ouchi, K. Aratsua and S. Yagai, *Chem. Commun.*, 2017, **53**, 9663.
- 47 G. M. Whitesides, E. E. Simanek, J. P. Mathias, C. T. Seto, D. N. Chin, M. Mammen and D. M. Gordo, *Acc. Chem. Res.*, 1995, **28**, 37.
- 48 D. C. Sherrington and K. A. Taskinen, *Chem. Soc. Rev.*, 2001, **30**, 83.
- 49 R. L. Beingessner, Y. Fan and H. Fenniri, *RSC Adv.*, 2016, **6**, 75820.
- 50 J. L. Sessler, C. M. Lawrence and J. Jayawickramarajah, *Chem. Soc. Rev.*, 2007, **36**, 314.
- 51 M. Fathalla, C. M. Lawrence, N. Zhang, J. L. Sessler and J. Jayawickramarajah, *Chem. Soc. Rev.*, 2009, **38**, 1608.
- 52 S. Sivakova and S. J. Rowan, *Chem. Soc. Rev.*, 2005, **34**, 9.
- 53 G. M. Peters and J. T. Davis, *Chem. Soc. Rev.*, 2016, **45**, 3188.
- 54 W. L. Jorgensen and J. Pranata, *J. Am. Chem. Soc.*, 1990, **112**, 2008.
- 55 J. Sartorius and H.-J. Schneider, *Chem. Eur. J.*, 1996, **2**, 1446.
- 56 A. Dunger, H.-H. Limbach and Klaus Weisz, *J. Am. Chem. Soc.*, 2000, **122**, 10109.
- 57 E. M. Todd, J. R. Quinn, T. Park and S. C. Zimmerman, *Isr. J. Chem.*, 2005, **45**, 381.
- 58 A. Likhitsup, R. J. Deeth, S. Otto and A. Marsh, *Org. Biomol. Chem.*, 2009, **7**, 2093.
- 59 M. J. Mayoral, J. Camacho-García, E. Magdalena-Estirado, M. Blanco-Lomas, E. Fadaei, C. Montoro-García, D. Serrano-Molina and D. González-Rodríguez, *Org. Biomol. Chem.*, 2017, **15**, 7558.
- 60 J. L. Sessler, D. Magda and H. Furuta, *J. Org. Chem.*, 1992, **57**, 818.
- 61 J. L. Sessler and R. Wang, *J. Am. Chem. Soc.*, 1996, **118**, 9808.
- 62 J. L. Sessler and R. Wang, *Angew. Chem. Int. Ed.*, 1998, **37**, 1726.
- 63 J. L. Sessler and R. Wang, *J. Org. Chem.*, 1998, **63**, 4079.
- 64 A. Marsh, M. Silvestri, J.-M. Lehn, *Chem. Commun.*, 1996, **13**, 1527.
- 65 M. Mascal, N. M. Hext, R. Warmuth, M. H. Moore and J. P. Turkenburg, *Angew. Chem. Int. Ed.*, 1996, **35**, 2204.
- 66 M. Mascal, N. M. Hext, R. Warmuth, J. R. Arnall-Culliford, M. H. Moore and J. P. Turkenburg, *J. Org. Chem.*, 1999, **64**, 8479.
- 67 M. Mascal, S. C. Farmer and J. R. Arnall-Culliford, *J. Org. Chem.*, 2006, **71**, 8146.
- 68 H. Fenniri, K. W. Temburnikar, R. S. Johnson, Reference Module in *Chemistry, Molecular Sciences and Chemical Engineering*, from Comprehensive Supramolecular Chemistry II, 2017, p. 83.
- 69 R. S. Johnson, T. Yamazaki, A. Kovalenko and H. Fenniri, *J. Am. Chem. Soc.*, 2007, **129**, 5735.
- 70 U. D. Hemraz, M. El-Bakkari, T. Yamazaki, J.-Y. Cho, R. L. Beingessner and H. Fenniri, *Nanoscale*, 2014, **6**, 9421.
- 71 L. Shuai, V. Parthasarathy, J.-Y. Cho, T. Yamazaki, R. L. Beingessner and H. Fenniri, *MRS Proceedings*, 2015, **1737**.
- 72 G. Borzsonyi, R. L. Beingessner, T. Yamazaki, J.-Y. Cho, A. J. Myles, M. Malac, R. Egerton, M. Kawasaki, K. Ishizuka, A. Kovalenko and H. Fenniri, *J. Am. Chem. Soc.*, 2010, **132**, 15136.
- 73 A. Asadi, B. O. Patrick and D. M. Perrin, *J. Am. Chem. Soc.*, 2008, **130**, 12860.
- 74 H. M. Keizer, J. J. González, M. Segura, P. Prados, R. P. Sijbesma, E. W. Meijer and J. de Mendoza, *Chem. Eur. J.*, 2005, **11**, 4602.
- 75 F. H. Beijer, R. P. Sijbesma, H. Kooijman, A. L. Spek and E. W. Meijer, *J. Am. Chem. Soc.*, 1998, **120**, 6761.
- 76 S. H. M. Söntjens, R. P. Sijbesma, M. H. P. van Genderen and E. W. Meijer, *J. Am. Chem. Soc.*, 2000, **122**, 7487.
- 77 B. J. B. Folmer, R. P. Sijbesma, H. Kooijman, A. L. Spek and E. W. Meijer, *J. Am. Chem. Soc.*, 1999, **121**, 9001.
- 78 A. Tessa ten Cate, P. Y. W. Dankers, H. Kooijman, A. L. Spek, R. P. Sijbesma and E. W. Meijer, *J. Am. Chem. Soc.*, 2003, **125**, 6860.
- 79 A. Tessa ten Cate, H. Kooijman, A. L. Spek, R. P. Sijbesma and E. W. Meijer, *J. Am. Chem. Soc.*, 2004, **126**, 3801.
- 80 A. Tessa ten Cate, P. Y. W. Dankers, R. P. Sijbesma and E. W. Meijer, *J. Org. Chem.*, 2005, **70**, 5799.
- 81 A. Zafar, S. J. Geib, Y. Hamuro and A. D. Hamilton, *New J. Chem.*, 1998, **22**, 137.
- 82 M. Saunders and J. B. Hyne, *J. Chem. Phys.*, 1958, **29**, 1319.
- 83 F. Rakotondradany, M. A. Whitehead, A.-M. Lebuïs and H. F. Sleiman, *Chem. Eur. J.*, 2003, **9**, 4771.
- 84 J. T. Davis, *Angew. Chem. Int. Ed.*, 2004, **43**, 668.
- 85 J. T. Davis and G. P. Spada, *Chem. Soc. Rev.*, 2007, **36**, 296.
- 86 S. Lena, S. Masiero, S. Pieraccini and G. P. Spada, *Chem. Eur. J.*, 2009, **15**, 7792.
- 87 G. M. Peters and J. T. Davis, *Chem. Soc. Rev.* 2016, **45**, 3188.
- 88 J. E. Betancourt, M. Martín-Hidalgo, V. Gubala and J. M. Rivera, *J. Am. Chem. Soc.*, 2009, **131**, 3186.

- 89 D. González-Rodríguez, J. L. J. van Dongen, M. Lutz, A. L. Spek, A. P. H. J. Schenning, E. W. Meijer, *Nature Chem.*, 2009, **1**, 151.
- 90 K. B. Sutyak, P. Y. Zavalij, M. Robinson and J. T. Davis, *Chem. Commun.*, 2016, **52**, 11112.
- 91 E. Fadaei, M. Martín-Arroyo, M. Tafazzoli and D. González-Rodríguez, *Org. Lett.*, 2017, **19**, 460.
- 92 J. L. Sessler, M. Sathiosatham, K. Doerr, V. Lynch and K. A. Abboud, *Angew. Chem. Int. Ed.*, 2000, **39**, 1300.
- 93 Y. Inui, M. Shiro, S. Fukuzumi and T. Kojima, *Org. Biomol. Chem.*, 2013, **11**, 758.
- 94 C. Fraschetti, M. Montagna, L. Guarcini, L. Guidoni and A. Filippi, *Chem. Commun.*, 2014, **50**, 14767.
- 95 F. W. Kotch, V. Sidorov, Y.-F. Lam, K. J. Kayser, H. Li, M. S. Kaucher, and J. T. Davis, *J. Am. Chem. Soc.*, 2003, **125**, 15140.
- 96 M. Nikan and J. C. Sherman, *Angew. Chem. Int. Ed.*, 2008, **47**, 4900.
- 97 M. Nikan and J. C. Sherman, *J. Org. Chem.*, 2009, **74**, 5211.
- 98 G. A. L. Bare, B. Liu and J. C. Sherman, *J. Am. Chem. Soc.*, 2013, **135**, 11985.
- 99 A. Laguerre, L. Stefan, M. Larrouy, D. Genest, J. Novotna, M. Pirrotta and D. Monchaud, *J. Am. Chem. Soc.*, 2014, **136**, 12406.
- 100 Y. Inui, S. Fukuzumi and T. Kojima, *Dalton Trans.*, 2013, **42**, 3779.
- 101 R. Otero, M. Schöck, L. M. Molina, E. Lægsgaard, I. Stensgaard, B. Hammer and F. Besenbacher, *Angew. Chem. Int. Ed.*, 2005, **44**, 2270.
- 102 A. Ciesielski, S. Lena, S. Masiero, G. P. Spada and P. Samorì, *Angew. Chem. Int. Ed.*, 2010, **49**, 1963.
- 103 M. El Garah, R. C. Perone, A. S. Bonilla, S. Haar, M. Campitiello, R. Gutierrez, G. Cuniberti, S. Masiero, A. Ciesielski and P. Samorì, *Chem. Commun.*, 2015, **51**, 11677.
- 104 D. González-Rodríguez, P. G. A. Janssen, R. Martín-Rapún, I. De Cat, S. De Feyter, A. P. H. J. Schenning and E. W. Meijer, *J. Am. Chem. Soc.*, 2010, **132**, 4710.
- 105 J. C. Chaput and C. Switzer, *Proc. Natl. Acad. Sci. U. S. A.*, 1999, **96**, 10614.
- 106 V. Abet and R. Rodriguez, *New J. Chem.*, 2014, **38**, 5122.
- 107 M. Meyer and J. Suhnel, *J. Phys. Chem. A*, 2003, **107**, 1025.
- 108 J. Gu and J. Leszczynski, *J. Phys. Chem. B*, 2003, **107**, 6609.
- 109 J. T. Davis, S. Tirumala, J. R. Jenssen, E. Radler and D. Fabris, *J. Org. Chem.*, 1995, **60**, 4167.
- 110 F. Seela and C. Wei, *Chem. Commun.*, 1997, 1869.
- 111 E. Orentas, C.-J. Wallentin, K.-E. Bergquist, M. Lund, E. Butkus and K. Wärnmark, *Angew. Chem. Int. Ed.*, 2011, **50**, 2071.
- 112 Q. Shi, K.-E. Bergquist, R. Huo, J. Li, M. Lund, R. Vácha, A. Sundin, E. Butkus, E. Orentas and K. Wärnmark, *J. Am. Chem. Soc.*, 2013, **135**, 15263.
- 113 D. Račkauskaitė, R. Gegevičius, Y. Matsuo, K. Wärnmark and E. Orentas, *Angew. Chem. Int. Ed.*, 2016, **55**, 208.
- 114 Q. Shi, T. Javorskis, K.-E. Bergquist, A. Ulčinas, G. Niaura, I. Matulaitienė, E. Orentas and K. Wärnmark, *Nat. Comm.*, 2017, **8**, 14943.
- 115 Q. Chen, X. Su, E. Orentas and Q. Shi, *Org. Chem. Front.*, 2019, **6**, 611.
- 116 A. Neniškis, D. Račkauskaitė, Q. Shi, A. J. Robertson, A. Marsh, A. Ulčinas, R. Valiokas, S. P. Brown, K. Wärnmark and E. Orentas, *Chem. Eur. J.*, 2018, **24**, 14028.
- 117 R. Chamorro, L. de Juan-Fernández, B. Nieto-Ortega, M. J. Mayoral, S. Casado, L. Ruiz-González, E. M. Pérez and D. González-Rodríguez, *Chem. Sci.*, 2018, **9**, 4176.
- 118 Y. Yang, M. Xue, L. J. Marshall and J. de Mendoza, *Org. Lett.*, 2011, **13**, 3186.
- 119 L. J. Marshall and J. de Mendoza, *Org. Lett.*, 2013, **15**, 1548.
- 120 Y. Yang, M. Xue, J.-F. Xiang and C.-F. Chen, *J. Am. Chem. Soc.*, 2009, **31**, 12657–12663.
- 121 Y. Yang, F. Huang, C.-F. Chen, M. Xia, Q. Cai, F.-J. Qian and J. Xiang, *Sci. Rep.*, 2013, **3**, 1059.
- 122 C. Montoro-García, J. Camacho-García, A. M. López-Pérez, N. Bilbao, S. Romero-Pérez, M. J. Mayoral and D. González-Rodríguez, *Angew. Chem. Int. Ed.*, 2015, **54**, 6780.
- 123 S. Romero-Pérez, J. Camacho-García, C. Montoro-García, A. M. López-Pérez, A. Sanz, M. J. Mayoral and D. González-Rodríguez, *Org. Lett.*, 2015, **17**, 2664.
- 124 C. Montoro-García, J. Camacho-García, A. López-Pérez, M. J. Mayoral, N. Bilbao, D. González-Rodríguez, *Angew. Chem. Int. Ed.*, 2016, **55**, 223.
- 125 M. J. Mayoral, J. Camacho-García, E. Magdalena-Estirado, M. Blanco-Lomas, E. Fadaei, D. Serrano-Molina and D. González-Rodríguez, *Chem. Sci.*, 2018, **9**, 7809.
- 126 C. Montoro-García, M. J. Mayoral, R. Chamorro and D. González-Rodríguez, *Angew. Chem. Int. Ed.*, 2017, **56**, 15649.
- 127 I. Cacelli and G. Prampolini, *J. Phys. Chem. A*, 2003, **107**, 8665.
- 128 E. Masson, *Org. Biomol. Chem.*, 2013, **11**, 2859.
- 129 C. Montoro-García, N. Bilbao, Iris M. Tsagri, F. Zaccaria, M. J. Mayoral, C. F. Guerra and D. González-Rodríguez, *Chem. Eur. J.*, 2018, **24**, 11983.
- 130 T. Xiao, X. Feng, S. Ye, Y. Guan, S.-L. Li, Q. Wang, Y. Ji, D. Zhu, X. Hu, C. Lin, Y. Pan and L. Wang, *Macromolecules*, 2012, **45**, 9585.
- 131 T. Xiao, S.-L. Li, Y. Zhang, C. Lin, B. Hu, X. Guan, Y. Yu, J. Jiang and L. Wang, *Chem. Sci.*, 2012, **3**, 1417.
- 132 X.-Z. Wang, X.-Q. Li, X.-B. Shao, X. Zhao, P. Deng, X.-K. Jiang, Z.-T. Li and Y.-Q. Chen, *Chem. Eur. J.*, 2003, **9**, 2904.
- 133 G. B. W. L. Ligthart, Haruki Ohkawa, Rint P. Sijbesma and E. W. Meijer, *J. Am. Chem. Soc.*, 2005, **127**, 810.
- 134 M. Suarez, J.-M. Lehn, S. C. Zimmerman, A. Skoulios and B. Heinrich, *J. Am. Chem. Soc.*, 1998, **120**, 9526.
- 135 H. Abe, M. Takase, Y. Doi, S. Matsumoto, M. Furusyo and M. Inouye, *Eur. J. Org. Chem.*, 2005, 2931.
- 136 N. Bilbao, I. Destoop, S. De Feyter and D. González-Rodríguez, *Angew. Chem. Int. Ed.*, 2016, **55**, 659.
- 137 J. Camacho-García, C. Montoro-García, A. M. López-Pérez, N. Bilbao, S. Romero-Pérez and D. González-Rodríguez, *Org. Biomol. Chem.*, 2015, **13**, 4506.
- 138 N. Bilbao, V. Vázquez-González, M. T. Aranda and D. González-Rodríguez, *Eur. J. Org. Chem.*, 2015, 7160.
- 139 J. A. Zerkowski, C. T. Seto and G. M. Whitesides, *J. Am. Chem. Soc.*, 1992, **114**, 5473.
- 140 L. J. Prins, D. N. Reinhoudt and P. Timmerman, *Angew. Chem. Int. Ed.*, 2001, **40**, 2382.
- 141 N. Kimizuka, T. Kawasaki, K. Hirata and T. Kunitake, *J. Am. Chem. Soc.*, 1995, **117**, 6360.
- 142 S. Yagai, Y. Goto, X. Lin, T. Karatsu, A. Kitamura, D. Kuzuhara, H. Yamada, Y. Kikkawa, A. Saeki and S. Seki, *Angew. Chem. Int. Ed.* 2012, **51**, 6643.
- 143 M. Pappmeyer, C. A. Vuilleumier, G. M. Pavan, K. O. Zhurov and K. Severin, *Angew. Chem. Int. Ed.*, 2016, **55**, 1685.